Review Article

Mohamed Madani, Shimaa Hosny, Dalal Mohamed Alshangiti, Norhan Nady, Sheikha A. Alkhursani, Huda Alkhaldi, Samera Ali Al-Gahtany, Mohamed Mohamady Ghobashy, and Ghalia A. Gaber*

Green synthesis of nanoparticles for varied applications: Green renewable resources and energy-efficient synthetic routes

https://doi.org/10.1515/ntrev-2022-0034
received November 14, 2021; accepted January 3, 2022

Abstract: This study presents an outline of the 12 principles of green relevance in nanomaterial synthesis. The goal of using green renewable resources is to protect the environment from negative effects, which can be achieved *via* several main directions, including the choice of innocuous solvents, such as supercritical (SC) fluids or water, and/or additives (*i.e.* stabilizers, capping, and reducing agents) such as polysaccharides, using alternative reaction circumstances, and the development of energy-efficient synthetic methods. This review shows how different green renewable resources routes are reducing the impact of chemical processes on the environment and how their benefit can be achieved in nanotechnology applications such as green energy.

Keywords: green chemistry, nanomaterial synthesis, 12 principles, environment, sustainability, gamma irradiation

Abbreviations

CS	chitosan
CTAB	cetyltrimethylammonium bromide
CTAC	cetyltrimethylammonium chloride
CCR2	C–C chemokine receptor type 2
DI	deionized water
EU	European commission
FT-IR	fourier-transform infrared spectroscopy
HOMO	a polymer made from many copies of a single repeating unit
IL-1β	interleukin 1 beta
InP	indium phosphide
NDs	nanodiamonds
pDNA/MNPs	plasmid DNA/Magnetic nanoparticles
PbS	lead(II) sulfide
ROS	reactive oxygen species
TEM	transmission electron microscopy
TFILs	thiol-functionalized ionic liquids
TNF	tumor necrosis factor

1 Introduction

Green chemistry is defined as the "design of chemical products and procedures for reducing or removing the using and production of harmful substances" [1,2]. This description and the green chemistry principles (GCP) in nanomaterial synthesis produced functional nanomaterial with minimal waste level. Production of nanomaterial benefits from the green approaches such as sugars, vitamins, and plants or agricultural waste that can revel as biodegradable capping and reducing agent. Raveendran *et al.* [3] were the first to establish the idea of green nanoparticles (NPs) production, using D-glucose as a reducing agent and starch as a capping agent to create starch silver nanoparticles (AgNPs). In addition, natural polysaccharide such

* **Corresponding author: Ghalia A. Gaber,** Department of Chemistry, Faculty of Science (Girls), Al-Azhar University, P.O. Box: 11754, Yousef Abbas Str., Nasr City, Cairo, Egypt,
e-mail: ghaliaasaid@azhar.edu.eg
Mohamed Madani, Dalal Mohamed Alshangiti,
Sheikha A. Alkhursani, Huda Alkhaldi: Collage of Science and Humanities-Jubail, Imam Abdulrahman Bin Faisal Univeristy, Jubail, Saudi Arabia
Shimaa Hosny: Chemistry Department, Faculty of Science, New Valley University, El-Kharga, 72511, Egypt
Norhan Nady: Polymeric Materials Research Department, City of Scientific Research and Technological Applications (SRTA-city), New Borg El-Arab city, Alexandria 21934, Egypt
Samera Ali Al-Gahtany: Faculty of Science, University of Jeddah, Jeddah, Saudi Arabia
Mohamed Mohamady Ghobashy: Radiation Research of Polymer Department, National Center for Radiation Research and Technology (NCRRT), Atomic Energy Authority, P.O. Box. 29, Nasr City, Cairo, Egypt

as gum arabic [4], chitosan [5], gumKondagogu [6], Acacia [7], and heparin [8] were also used to make AgNPs. The (1) stabilizing agent, (2) reducing agent, and (3) solvent should all be considered while developing a green technique for NP production [9].

Green chemistry is built on 12 principles proposed by Paul Anastas and John Warner, who tried to describe a greener (or more environment friendly) chemical process or product [10]. The GCP were developed for the pollution prevention before occurring it from its source by reducing the usage of harmful chemicals in nanomaterial preparation. The application of the twelve principles of green chemistry in nanoparticle synthesis is a relatively new emerging issue related to sustainability. The field has received a lot of attention in recent years due to its ability to design alternative, safer, energy efficient, and less toxic methods towards synthesis. These pathways have been associated with the rational use of different materials in nanoparticle preparations and synthetic methods [11,12]. Figure 1 summarized 12 principles of green chemistry with a corresponding green nanotechnology approach.

The structural features of nanomaterials, such as size, structure, composition, and surface chemistry, are critical for their use in various catalytic, electronics, biology and biomedical applications, material science, physics, environmental remediation, and interdisciplinary fields, as well as their toxicity. To expand the range of characteristics, various environmentally acceptable methods leading to NPs of diverse shapes and sizes relevant to a particular application must be developed. This article will review the current state of the art in the use of biodegradable homo and block copolymers such as polysaccharides, as well as enzymes, to manufacture a variety of nanomaterials by controlling three parameters. The stabilizing agent, the reducing agent, and the solvent should all be considered. Gamma irradiation techniques have several advantages when compared to alternative methodologies or conventional technologies such as gives superior yields and monodisperse of nanometallic clusters. Other advantages and potential of gamma irradiation synthesis involve performing studies at mild pressure and temperature conditions, without the need of chemical reducing agents, and with good reproducibility. The use of experimental methods allows for the manufacture of NPs of high grade without the use of chemical reducing agents, as well as the regulation of particle size and morphology. Another advantageous feature of this method is its adaptability with respect to radiation sources as it may be carried out using gamma, e-beam, and X-rays without compromising the end product or requiring composition adjustments, apart from modifying the radiation source. The ability to combine sterilization with NP production in a single operation is a unique benefit that ionising radiation may provide. Particularly, when comparing with other methods for the NP synthesis and other nanomaterial synthesis, this process takes place by having a simultaneous effect on pathogenic or contaminating microorganisms and the material or ions that leads to the formation of NP in a much faster, simpler, and cost-effective method. If the irradiation procedure is correctly done and controlled, there should be no byproducts or significant harm to the product. This benefit is even more significant if the created system matches to the final product to be sold because radiation may be done inside the final package, preventing further contamination and very low handling.

2 Polysaccharide stabilizing agents

The high chemical activity of nanostructured materials with a developed surface is frequently the source of undesirably strong and often irreversible reactions such as aggregation. Aggregation decreases NP activity by reducing the surface area and interfacial free energy. Stabilizing agents such as polysaccharide molecules are frequently low toxic and used, from the environmental perspective, in colloidal synthesis of NP to restrict particle size evolution, control particle shape, and shield or passivate the surface against aggregation. Thus, increasing the stability of the synthesized NP throughout storage, transportation, and its full life cycle is very important. The majority of stabilization methods, as emphasized by Stubbs and Gilman [13], involve dispersant molecules such as surfactants or polyelectrolytes, which not only change the chemistry and physics of the surface of NPs but also produce a big waste stream even though they make up a significant (more than 50%) mass fraction of a NP system. As a consequence, there is a need to find environmentally harmless stabilization and functionalization routes as well as biodegradable, that is, non-immunogenic, non-toxic, and hydrophilic stabilizing agents to minimize contamination and consequent negative impacts on the environment.

There are already a number of “green” stabilizing agents available, such as biodegradable polymers (polysaccharides), to mention a few, that can be stable and functionalize nanomaterials without causing harm to the environment or biosystems. Considering the enormous quantity of information accessible, this review will be limited to the application of biodegradable polymers in the stabilization of nanomaterials. The synthesized NPs are prevented from aggregating by the complex network

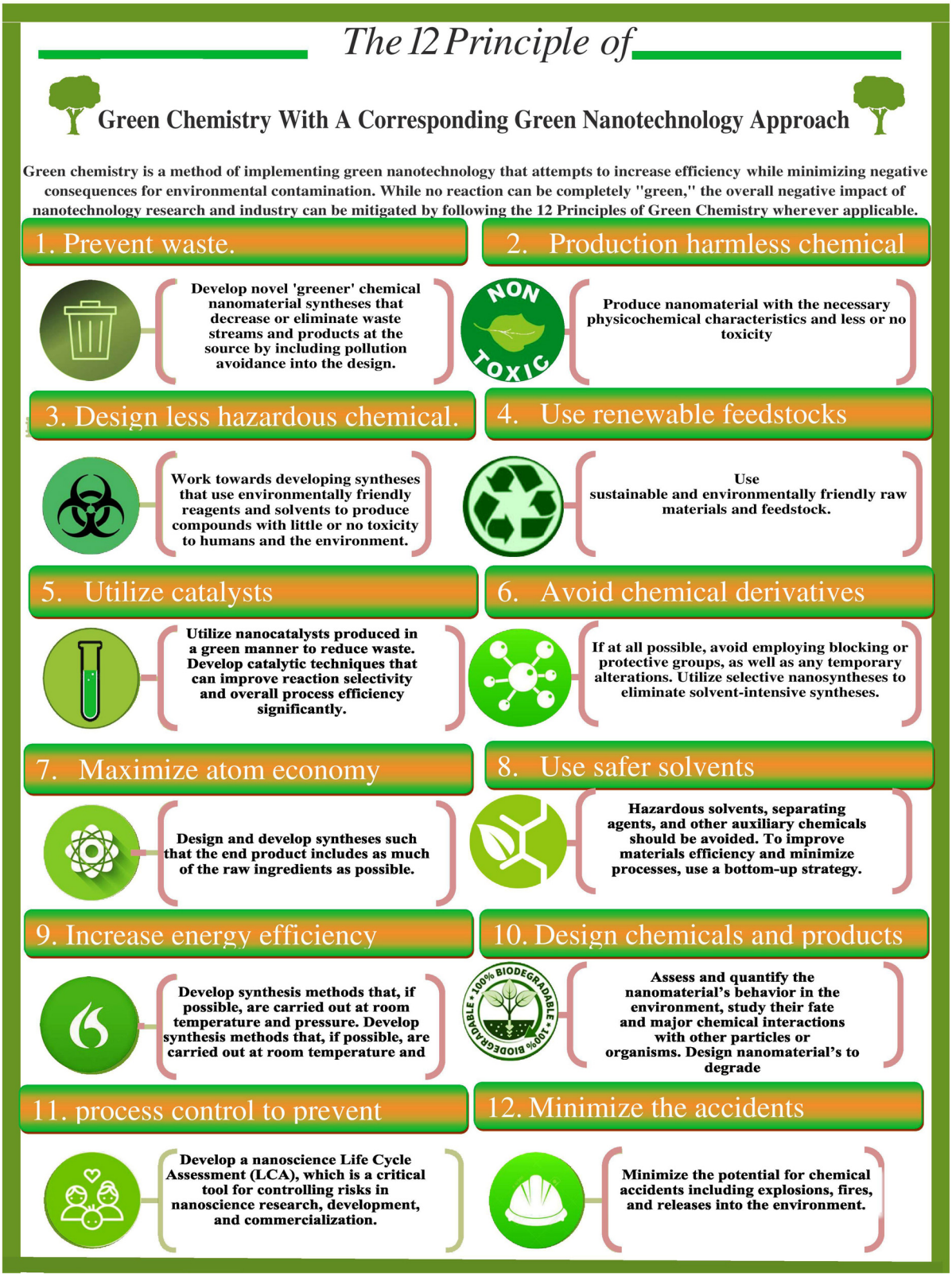

Figure 1: Twelve principles of green chemistry and the corresponding green nanotechnology approach.

formation by intermolecular hydrogen bonds associated with the polysaccharide framework. However, in order to enhance the solubility of polysaccharides such as starch in reaction mixtures, high temperatures are usually required, resulting in the reduction of precursors prior to complexation between precursors and polysaccharides. The full functionality of capping agents in regulating the production of NPs could not be realized in these situations. High water solubility of polysaccharides at moderate temperatures is necessary to enhance the loading quantity of precursors before they decrease to NPs. In some cases, starch can act as both stabilizing and reducing agent. For example, AgNPs could be obtained by the reduction of Ag ions using starch as a reducing and capping agent [14]. High water solubility of polysaccharides at room temperature is necessary to enhance the loading amount of precursors before they decrease to NPs. This was accomplished with the help of dextran (Dex), which was used as a biocompatible stabilizing agent for the production of nanoscaled particles.

2.1 Dextran

Dextran is a polysaccharide composed mostly of a-D-glucopyranosyl units with variable chain lengths and branching patterns. It may be used to cover a variety of metallic and non-metallic NPs as it is very biocompatible, non-toxic, and hydrophilic. It is made biotechnologically on a large scale using Leuconostoc mesenteroides and a variety of different bacteria strains. Because of its biocompatibility and biodegradability, the biopolymer is frequently used in biomedical fields due to its increased drug loading capacity in the host NPs [15]. In addition, the peptide was attached to the Dex surface by establishing an oxime bond between its alkoxyamino group and the reducing end of the Dex [16].

Banerjee *et al.* [17] synthesized Dex exopolysaccharide (Dex-EPS) by a geothermal spring origin *Bacillus anthracis* PFAB2. The Dex-EPS is used for the green synthesis of AgNPs. Currently, because environmental toxicity is a problem, experts are focusing on developing an environmentally friendly procedure. Given the risks inherent with the chemical NP synthesis, green synthesis methodologies have received a lot of interest for their long-term viability in nanomedicine and bioengineering. According to TEM analysis, the AgNP in Dex-EPS/AgNPs has a hexagonal form with a diameter of 84 nm. When compared to traditional antimicrobials, the Dex-EPS/AgNPs showed promising biocidal characteristics for both gram-positive and gram-negative bacteria, as well as several potentially dangerous fungi.

İspirli *et al.* [18] prepared AgNPs (10 nm) in neutral aqueous solutions (pH 7) of 0.4% w/v $AgNO_3$ in the presence of 0.3% v/w Dex. The mixture solution was put in 15 psi pressure and 120°C of autoclave to assist the reduction reaction of $AgNO_3$ using Dex as a stabilizing agent. Authors produced Dex from *Weissella cibaria* and studied the anti-microbial and anti-fungal activities of the obtained product of AgNPs-Dex. The obtained results show that 1 mg mL^{-1} of AgNPs-Dex was sufficient for the anti-fungal activity against *Fusarium oxysporum*, *Alternaria alternata*, *Aspergillus niger*, *Penicillium chrysogenum*, and *Aspergillus parasiticus* and antibacterial activity against *Staphylococcus aureus*, *Yersinia enterocolitica*, *Bacillus cereus*, *Escherichia coli*, and *Salmonella typhimurium*.

Ashtiyani *et al.* [19] fabricated non-viral gene carriers based on Dex-stearic acidspermine (DSASP) amphiphilic polymer with validated lipid and amine conjugations that were linked with Fe_3O_4 NPs (12–18 nm) to increase target transport and shorten transfection time utilizing a static magnetic field. Non-viral gene carriers have shown significant promise in gene transport due to their low negative effects, improved bioavailability, permeability, and potential benefit of electrostatic interactions. The DSASP–pDNA/MNPs showed substantial pDNA condensation, resistance against DNase destruction, and significant cell survival in HEK 293T cells. In the presence of a high stearic acid content in DSASP polymer, another efficient factor in polymer size rate that leads to greater DNA condensation is the presence of stearic acid. Zhao *et al.* [20] synthesized acylated Dex-*g*-polyisobutylene (AcyDex-*g*-PIB) graft copolymers with varied branch lengths (Mn, PIB, 2,600–5,800 g mol^{-1}) and grafting numbers (GN, 5–28 per 1,000 Dex monosaccharide) as amphiphilic nanosphere polymer (500 nm) by nucleophilic substitution of the (–OH) and PIB-tetrahydrofuran (THF)4+ through cationic polymerization reactions. The amphiphilic AcyDex-*g*-PIB graft copolymers can self-assemble into nanospheres in aqueous medium, which could be used as pH-sensitive drug delivery carriers that could deliver 100% of the drug loading within 72 h at pH = 7.4. Furthermore, the antibacterial activities of AcyDex-*g*-PIB graft copolymers with Ag-NPs were tested against *E. coli* and *S. aureus* according to Kirby-Bauer method. The diameter of inhibition zone increases with increasing AgNPs content.

For vascular inflammation therapy, magnetic iron oxide core (Fe_3O_4; 7–10 nm) and shell of Dex with anti-inflammatory polyphenols loaded such as protocatechuic acid (PCA) were synthesized by Anghelache *et al.* [21]. Vascular inflammation is a key factor in the advancement of a variety of diseases, including atherosclerosis, and as a result, it has emerged as a promising therapeutic target. The obtained results confirmed that Fe_3O_4-Dex/PCA exhibited an exert activity of an anti-inflammatory at non-cytotoxic of PCA concentration (350 μM) as supported by the

reduced inflammatory molecule levels such as TNF-α, IL-1β, MCP-1, IL-6, and CCR2 in activated endothelial cells (ECs) and M1-type macrophages and functional monocyte adhesion assay. In EC and monocytes, the addition of Dex on its surface has been demonstrated to reduce iron oxide cytotoxicity [22].

Esfahani *et al.* [23] prepared gold nanoparticles (AuNPs) coated by mercaptoacetic acid (MA-AuNPs) as a colorimetric sensor for phosphate (P) detection in drinking water. The surface plasmon resonance (SPR) effect causes the colour of AuNPs to shift from blue to red throughout the aggregation and disaggregation processes, with europium ions (Eu^{3+}) functioning as the aggregating agent in this sensor. Dex is used to encapsulate the Eu^{3+} ions into a tablet form to make the detection technique more easily. As a consequence, the sensor is work simple by dissolving a Eu^{3+}-Dex tablet in water and then adding MA-AuNPs to detect P colorimetrically. The detection limit of this test has been established to be 0.3 g L^{-1} with a higher detection limit of 26 g L^{-1}, whereas the permissible limit of P in drinking water is 10 g L^{-1}.

Kokilavani *et al.* [24] used tyrosine and nanocomposite of Cu/Ag-Dex (26 nm) to construct a cheap colorimetric sensor for detection of Hg^{2+} in aqueous solution. Mercury is one of the most dangerous metal contaminants, posing a catastrophic hazard to the environment and human health even at very low levels.

Bevacqua *et al.* [25] prepared Dex–curcumin NPs of 290 nm for the delivery of anticancer drugs of prostate cancer in combination with Doxorubicin (DOXO). Functional nanocarriers that can effectively vectorize pharmaceuticals to the region of interest while also acting as cytotoxic agents are a big step forward in the hunt for effective anticancer methods with minimal side effects than the traditional chemotherapeutics. Due to NPs, DOXO release was pH-dependent, with more efficient release in acidic circumstances, and immobilizing curcumin in Dex NPs dramatically increased the curcumin efficiency. At low dosages, the IC_{50} was reduced by half, an apoptotic impact was created, and ROS production was improved (from 67 to 134%). Finally, a synergistic relationship between NPs and DOXO was discovered, with free curcumin and Dex demonstrating further effectiveness. In various studies, Dex (DOX-NPs), loaded with doxorubicin (DOX), was utilized as a model of a well-known anticancer medication.

El Founi *et al.* [26] used the emulsion-solvent evaporation process to synthesize doxorubicin-loaded NPs made of a poly(*o*-nitrobenzyl acrylate) and Dex shell in the presence of CuBr or $CuSO_4$/ascorbic acid that acts as a catalyst. UV irradiation technique was applied to release DOX on the Caco-2 cell viability. After 30 s UV irradiation, the amount of DOX released was 45%, reaching even 54% after 48 h. DOX-loaded NPs were then incubated with Caco-2 cells and then irradiated for 30 s is release 31 μM of DOX, which is close to the DOX IC_{50} value toward Caco-2 cells. In comparison, the diffusion out of DOX NPs (without irradiation) even after 48 h of incubation, does not provide such results.

Das *et al.* [27] created a one-pot synthesis for carboxymethyl-Dex coated (carboxymethyl cellulose [CMC]) and iron oxide (Fe_3O_4) NPs, called "CION", that may be used for functional mapping and sensitive structural of the cerebral blood volume (CBV) using magnetic resonance imaging (MRI). When delivered intravenously, supermagnetic iron oxide NPs are potent MRI contrast agents for sensitive structural and functional mapping of CBV. Feraheme, which is developed for the therapeutic treatment of iron deficiency, has been used in multiple CBV-MRI research thus far. Due to economic and regulatory constraints, Feraheme is currently unavailable outside of the United States, making CBV-MRI procedures either inaccessible or prohibitively expensive. To overcome this problem, CION's potential as a cross-modality research platform may be demonstrated by demonstrating simultaneous *in vivo* optical and MRI measurements of CBV utilizing fluorescent-labelled CION.

Several literatures used Dex to stabilize of (MRI) contrast agents. Popov *et al.* [28] prepare gadolinium-doped ceria nanoparticles $Ce_{0.9}Gd_{0.1}O_{1.95}$ exhibiting excellent colloidal stability due to dextran coating as MRI contrast agents with high T_1 relaxivity (3.6 mM^{-1} s^{-1}) and selective cytotoxicity *via* ROS generation to cancer cells. The viability of normal cells was not affected by the $Ce_{0.9}Gd_{0.1}O_{1.95}$ NPs, whereas a dose-dependent reduction in the MCF-7 cell viability was founded at high Dex-coated/$Ce_{0.9}Gd_{0.1}O_{1.95}$ nanocomposite concentrations of >0.3 mg mL^{-1}. This difference is most likely related to the development of mitochondrial-mediated apoptosis in cancer cells as Dex-coated/$Ce_{0.9}Gd_{0.1}O_{1.95}$ nanocomposite caused a substantial reduction in their mitochondrial membrane potential. The activation of the apoptosis mechanism in cancer cells in the presence of Dex-coated/$Ce_{0.9}Gd_{0.1}O_{1.95}$ nanocomposite was revealed by a significant increase in CD40 gene expression, indicating oxidative stress activation. In normal cells, incubation with Dex-coated/$Ce_{0.9}Gd_{0.1}O_{1.95}$ nanocomposite caused no changes in mitochondrial membrane potential while lowering ROS levels. Dex-coated/$Ce_{0.9}Gd_{0.1}O_{1.95}$ nanocomposite did not penetrate the nuclei and had no genotoxic effects in both normal and cancer cells.

Figure 2 shows the effect of Dex at concentration of 25, 100, 200, 500, and 1,000 μL as capped and stabilizing agent of the formed AuNPs as well as the identical UV-Vis spectrum of the obtained Dex-AuNPs. The TEM showed that an increase in Dex amount decreased the particle size. The average diameters of the obtained Dex-AuNPs were 25.86, 9.71, 9.59, 8.22, and 5.14 nm for adding (25, 100, 200, 500,

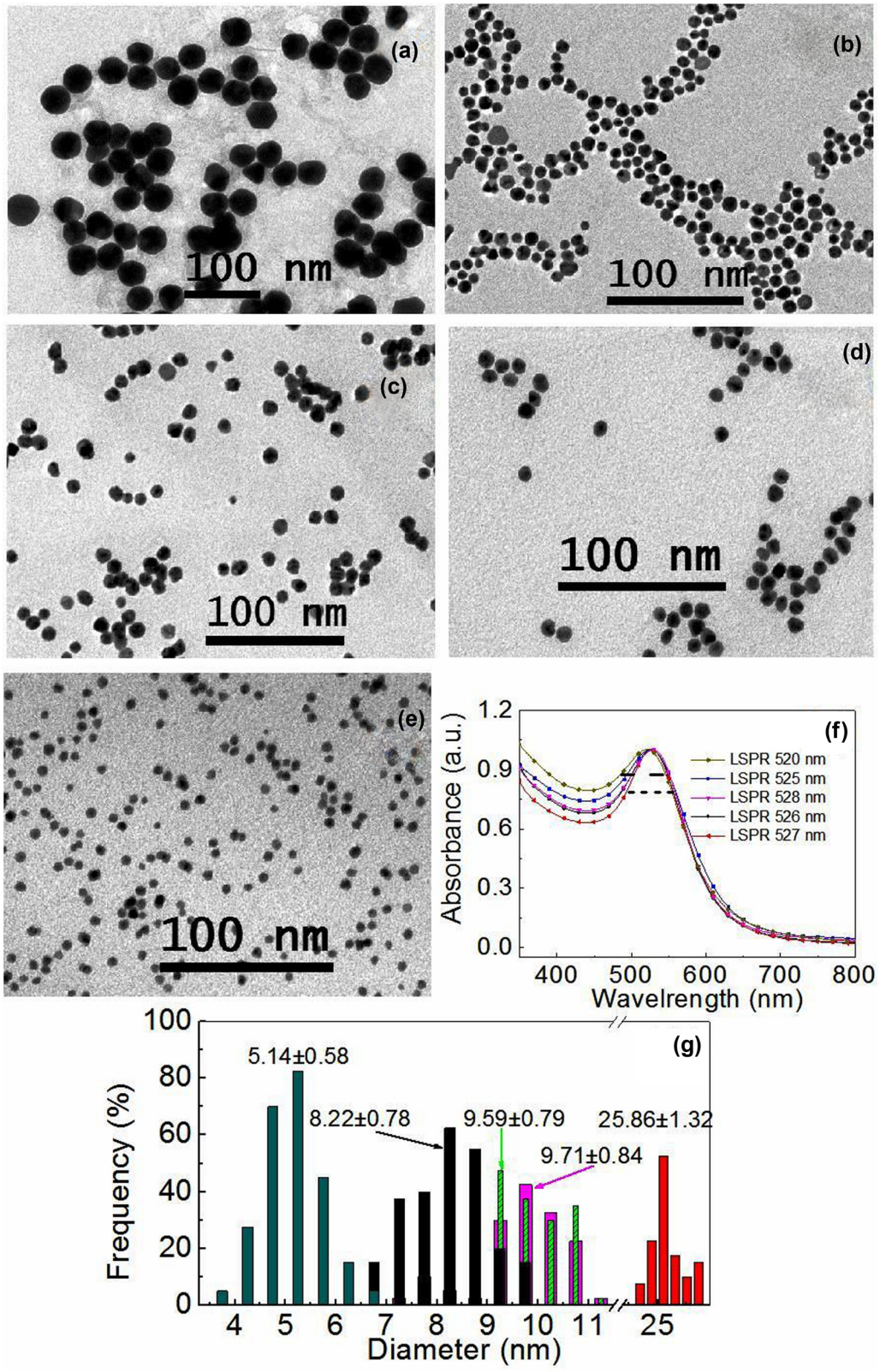

Figure 2: The TEM micrographs of Dex-AuNPs with different concentration of Dex (25, 100, 200, 500, and 1,000 µL) for (a–e) samples, respectively. (f) UV-Vis absorption spectra for the corresponding AuNPs [30]. (g) Particle size distributions of the TEM images; Copyright 2018, Elsevier.

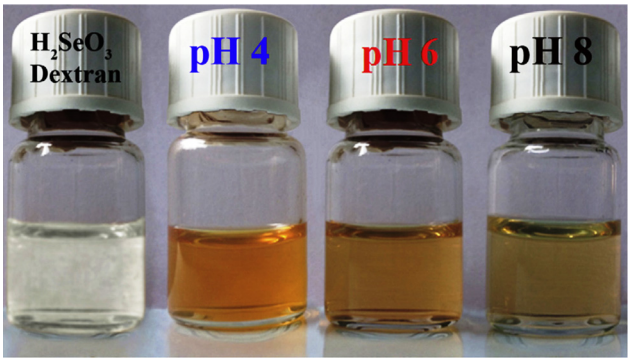

Figure 3: Photograph of un-irradiated H_2SeO_3/Dex solution and the gamma irradiation synthesized of SeNPs/Dex solutions at dose of 25 kGy and at different pHs (4, 6, and 8) ref. [31]; Copyright 2018, Elsevier.

and 1,000 µL) of Dex, respectively. The UV-Vis spectrum showed an overall blue shift of the maximum absorption peaks from 527 to 520 nm as the NP size was decreased as a result of increasing the amount of Dex. Figure 3 illustrates the γ Co-60 ray irradiation of H_2SeO_3/Dex solution at irradiation dose of 25 kGy to produce selenium nanoparticles (SeNPs) with a size of 74 nm. The colour of the 25 kGy of H_2SeO_3/Dex solution changed from colourless to orange-red, indicating that SeNPs were forming. In general, the gamma irradiation technique has been regarded as a green synthesis method capable of producing large-scale NPs [29].

2.2 Chitosan

Chitosan is an excellent stabilizer for the green production of metal NPs. Because of the non-covalent interactions between the surface of the metals, the metal NPs may easily aggregate in solution. However, chitosan is a steric barrier that surrounds the metal with a positive charge. The creation of homogenous metal NP solutions was enabled by the strong electrostatic repulsion between the positive-charge coated metal NPs. Chitosan has been shown to be effective for stabilizing metal NPs in several studies, as shown in Figure 4. TEM image shows porous flower-shaped palladium nanoparticles (PdNPs) synthesized by ascorbic acid reduction as green method and stabilized by chitosan. The size of the obtained flower-shaped PdNPs was discovered to be influenced by the amount of chitosan present. The flower-shaped PdNPs have great biocompatibility and stability [32]. 50 mg of vitamin C (VC) in 15 ml of water. Next, the different chitosan amount was used in concentration of 0.05, 0.067, 0.1, 0.133, 0.2, 0.4, and 0.6% to obtain different pH values of 3.01, 3.07, 3.12, 3.17, 3.26, 3.63, and 3.9, respectively. These results were lower than chitosan's pK (usually 6.5), thus 10 mL $HPdCl_4$ 0.01 M was added to the chitosan solution. The resulting NPs were flower shaped in nanoscale after 2 h. Centrifugation was used to collect the samples, which were subsequently washed three times with DI and dried in a vacuum. The identical process was utilized to make PdNPs for the control group, with the exception of adding CS. The resulting PdNPs were flower shaped but varied in size, according to TEM images. The NPs made with 0.05% (m/V) CS had size of 153.7 nm, which was almost larger than those made with 0.4 and 0.6% (m/V) with size of 30 and 25 nm. The findings revealed that the appropriate NP size may be easily achieved by altering the CS concentration.

Another example of chitosan as a size controller is green metal NP synthesis. Based on UV-visible spectroscopic data, Kalaivani *et al.* [33] found that the size of

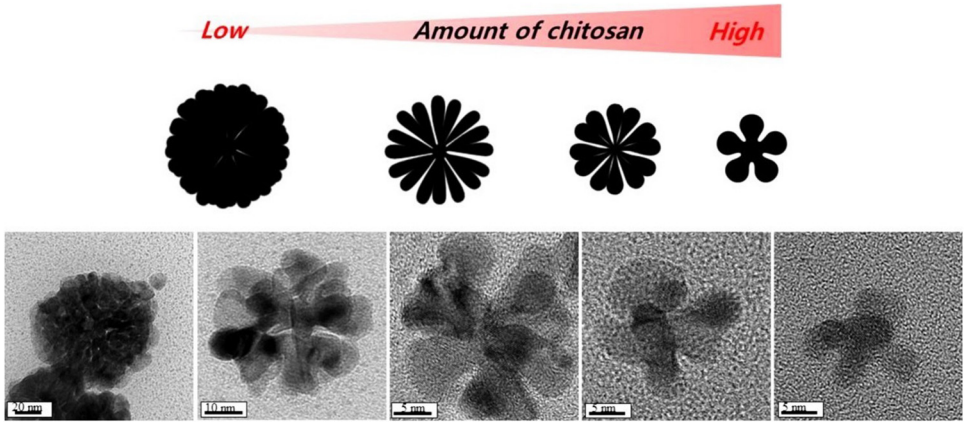

Figure 4: The TEM image of flower-shaped PdNPs, their size and shape dependence on the amount of chitosan. Ref. [32] Copyright 2019, Elsevier™.

AgNPs was effectively decreased as the amount of chitosan is increased. Furthermore, at lower chitosan content, the size of AgNPs was noticeably increased. This conclusion was again confirmed by our recent studies where the size of metal NPs decreasing when the concentration of chitosan was increased [34]. To understand how chitosan influences the size of produced NPs, researchers proposed a hypothesis. The positively charged chitosan has a significant electrostatic interaction with the metal nuclei during the production of metal NPs in the presence of chitosan. The stronger the connection between chitosan and the metal nuclei, the higher the concentration of chitosan. This strong contact prevents precursors from attaching to metal nuclei. In the presence of a high concentration of chitosan solution, metal nuclei are unable to develop any further [35].

Modifying the characteristics of chitosan for regulating the form and size of NPs might be beneficial for environment. Harmful capping agents (*e.g.* CTAB, CTAC, and trisodium citrate) are commonly used as shape-directing agents for metal NPs in the chemistry technique [34,36,37]. Replacing these compounds with natural products such as chitosan is an excellent way to improve metal NP biocompatibility for long-term biomedical uses. As described in an earlier study [38], thiolated chitosan may be utilized as a soft template for the production of gold nanochains, nanoneedles, and nanoflowers. Various shapes of AuNP assemblies, including 3D microclusters, microflowers, 2D needle-like crystals 1D chains, and single crystal microcubes, could be obtained by controlling the mercapto groups density (degree of substitution) on the modified chitosan. Luesakul *et al.* [39] summarized the routes of SeNP self-assembly with a cubic shape using three mixture of gallic acid–folic acid–*N*-trimethyl chitosan (GA–FA–TMC) as follows: (1) *via* the electrostatic interaction enhancement between the negatively charged surface of SeNPs and the positively charged surface of the stabilizer due to *N*-trimethyl chitosan ($N^+(CH_3)_3$), (2) *via* hydrophobic components of both gallic acid and folic acid, the formation of π–π stacking interaction with *N*-trimethyl chitosan, and (3) *via* the intermolecular H-bonding between the hydrophilic moieties of GA–FA–TMC. These three routes allows the self-assembly of SeNPs into cubic shape.

2.3 CMC

CMC is of an important polysaccharide stabilizer NPs because of the presence of negative charge on the CMC molecules. The charge on CMC molecules has a good influence on NP stabilization and makes colloidal stability easier to obtain [40,41]. Unlike cellulose, sodium salt of CMC is water-soluble although it is derived from cellulose molecules. CMC can be suitable in many bio-fields applications due to CMC having chemical structural stability and high mechanical properties at pH ranging from 3 to 10. A CMC solution is very viscous solution due to electrostatic interactions and intermolecular H-bonds between groups of hydroxyl and carboxylic through CMC molecules. The synergistic effect of inorganic and organic materials such as aluminium ion, glycerin, and cognac glucomannan is dependent on these electrostatic interactions. This method is suited for producing cellulose-based goods with desirable qualities that can fulfil industry's expanding demands [42,61]. However, since intermolecular H-bondings are disrupted, this CMC polymer loses stability of its structural and viscosity at pH levels of more than 10. Because noble metals, such as Au, Pt, and Pd, cannot bind with carboxyl groups of CMC at ambient temperature, CMC is unable to create NPs of them [43], whereas CMC can stabilize FeNPs in aqueous solutions independent of temperature [44]. Nadagouda and Varma [43] established a methodology using microwave irradiation (MW; 100°C, 5 min) and CMC as a capping and reducing agent to make homogeneous CMC-stabilized noble metal salt NPs with smaller diameters. MW of aqueous solutions of noble metal salts containing suitable quantities of CMC was used to create homogenous coloured nanocomposites with varied morphologies. Unusual Cu-CMC composites displayed needle-like nanostructures in the shape of bushes, and Fe showed evenly embedded spherical NPs in the CMC matrix, whereas Ag exhibited a spherical morphology with a predominance of cube-shaped NPs. Under MW, fully dispersed FeNPs were generated in aqueous solution under vacuum (reaction time approx. 30 min), and the obtained particles is stable for 9 days in the presence of a reducing agent sodium borohydride ($NaBH_4$). However, PdNPs synthesized in aqueous solution at temperatures of 22, 50, 80, and 95°C using CMC as a stabilizing agent and ascorbic acid as a reducing agent to give spherical nanostructures of Pd [45]. For the trichloroethene degradation in aqueous solutions, CMC-PdNPs showed a high catalytic reactivity regardless of their size [45]. Furthermore, Pt spherical NPs were stabilized for 9 months in aqueous solutions in the presence of CMC and $NaBH_4$ as the reducing agent [46]. As a result, it is acceptable to conclude that spherical metal NPs were generated when CMC was added as a stabilizing agent (independent of the existence or absence of the reducing agent).

Maslamani *et al.* [41] prepared nanocomposite beads of CMC/CuO-NiO stabilized by CMC by following the steps. Initially, of CMC 0.5 g was dissolved in deionized

water of 25 mL at temperature of 50°C with 2 h stirring to form homogenized solution of CMC. Then, 60 mg of mixed CuO-NiO (50:50) was dispersed in 5 mL deionized water and sonicated for 10 min. Then both CMC solutions were mixed and CuO-NiO dispersed at temperature of 50°C for 1 h, and then the homogeneous mixture was added dropwise into a the crosslinking solution of $FeCl_3$ (0.2 M) with stirring to form beads of CMC/CuO-NiO. Asghar *et al.* [47] used *Syzygium aromaticum* ethanolic buds extract as a reducing agent and CMC as a stabilizing agent in the green synthesis approach of AgNPs. The colloidal AgNPs were characteristic using a UV spectrophotometer for performed the successful synthesis of CMC-AgNPs. CMC-AgNPs UV-Vis spectrum shows numerous SPR bands at various wavelengths in the region of 400–420 nm, indicating the presence of a combination of CMC, AgNPs, and plant extract.

In order to fabricate AgNPs in aqueous solution, Khan *et al.* used sulfonated CMC (S-CMC) as an eco-friendly stabilizer agent [48]. The synthesis of AgNPs was investigated using UV-Vis spectra and typical SPR peak analysis. The UV-Vis spectra exhibits maximum absorbance (λ_{max}) at about ~400 nm owing to SPR of (S-CMC)-AgNPs nanobiocomposites. The obtained results showed that the low S-CMC concentration leads to widen SPR bands due to a low concentration of S-CMC, and there is no redox reaction among Ag + ions by S-CMC. However, at high S-CMC concentrations, the UV-Vis spectra exhibits maximum and sharp absorbance (λ_{max}) at about 390 nm owing to SPR of (S-CMC)-AgNPs. Increased concentration of S-CMC as stabilizing/reducing agent accelerated the formation of AgNP, resulting in a sharp SPR band. The formation of van der Waals forces between the S-CMC groups such as carboxyl and hydroxyl and the AgNPs resulted in the stability of AgNPs into nanobiocomposites.

Raghu Babu *et al.* investigated the effects of CMC concentrations on the production of PbS nanocrystals [49]. According to the FT-IR analysis, the interactions of hydroxyl (–OH) and carboxylate (–COO–) groups present in the CMC molecules appear to have a substantial role in the stabilization/capping of PbS nanocrystals, TEM analysis observations revealed that PbS nanocrystals generated with a little quantity of CMC (0.01% w/v) have aggregated nanowire networks created by the assembly of PbS NPs with random morphologies. However, aggregated nanowire networks were seen in PbS nanocrystals synthesized with a high level of CMC (0.1% w/v), but they were created by the assembly of rod-shaped PbS NPs.

3 Polysaccharide reducing agent

For NP manufacturing, polysaccharides such as xylan, mannan, glucomannans, and cellulose are regarded as "green" reducing agents. Because they contain aldehyde groups with OH groups of β-D-glucose unit, it allows polysaccharides to dissolve in water with high solubility and chelate with ions and reduce it in an alkaline medium (Figure 5), reducing the need for hazardous organic solvents. The above-mentioned four polysaccharides have β-D-glucose molecules that can act as a reducing agent. Also, some disaccharides are reducing sugars such as lactose, cellobiose, and maltose. Furthermore, certain oligosaccharides, which have a β 1 → 4 glycoside linkage, such as polysaccharides, operate as reducing agents. Glucose was widely utilized as a reducing agent in the synthesis of copper nanoparticles (CuNPs). This is owing to the existence of β-hemiacetal that convert to aldehyde groups at pH >8 leading to the reduction of dissolved ions and remaining of hydroxyl group in glucose that convert to gluconic acid (Figure 5).

Potentially, polysaccharide molecules containing aldehyde-end groups are referred to as green reducing agents. In an alkaline solution (pH >8), the aldehyde group act as an electron acceptor. The content of nonreducing to reducing moieties in polysaccharide is very important in NP synthesis. Although, there are around 300–600 distinct units of glucose in starch molecules, but only one terminal glucose unit possesses a hemiacetal. It takes more than one hemiacetal "needle" in a haystack of "acetals" to yield a positive sugar-reduction test. As expected, one hemiacetal unit is not enough to begin the reduction reactions, so starch is not classified as a reducing polysaccharide.

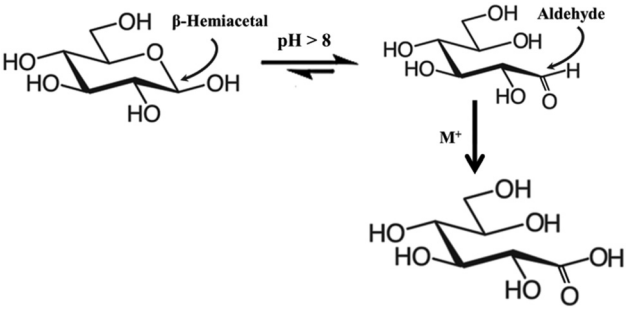

Figure 5: The adverse reducing reactivity of the cellulose molecule depends on the pH of aqueous solutions that leads to the tautomeric equilibrium between open-chain aldehyde and hemiacetal.

3.1 Xylan

Xylan, a polysaccharide made from xylose monomers, operates as a reducing agent for the production of sustainable NPs with a wide range of applications without the usage of harmful chemicals. Corn cob is an agriculture waste that generates tens of thousands of tonnes of garbage each year, but it is also an excellent source of a bioactive reducing polysaccharide, for example, xylan. Silva Viana *et al.* [50] used ultrasound to extract xylan from corn cob, which was verified by using NMR studies. The extracted xylan solution (10 mg mL^{-1}) was mixed with a 1.0 mM silver nitrate ($AgNO_3$) solution. After 24 h, the mixture colour changed to give brown suspension of silver nanoxylans (102 nm). It has been also reported that the extract of xylans from corn cobs dissolved in the solution of NaOH under ultrasonic assist by Brito *et al.* [51]. He and coauthors used the extract xylan as a stabilizing and reducing agent for AgNP production. Feng *et al.* [52] designed an electrochemical sensor based on gold-carbon dots nanocomposite Au@CQDs50 MXene for nitrite detection in water samples. The carbon dots were synthesized from polysaccharide xylan that also used as *in situ* green reducing agents of gold ions at alkaline media. Commonly, a single-layered graphene quantum dots (GQDs) are prepared from carbon precursors through a bottom–up strategy. Cai *et al.* [53] used xylan under hydrothermal conditions to fabricate a single-layered GQDs with the assistance of NaOH/urea. The self-passivated layer of xylan molecules on obtained GQDs surface displayed quantum yield of a fluorescence 23.8%. This passivated layer was destroyed and fluorescence quenching by strong oxidants ions such as Cr(VI) are attached with xylan molecules by nitrogen and oxygen functional groups. The finding results confirm the mutual oxidation reduction reactions between Cr(VI) and xylan molecules that candidate (GQDs)/xylan molecules to use as Cr(VI) detection.

Carbon quantum dots (CQDs) based on polysaccharide of xylan are also frequently used in the detecting ions applications, The majority of CQD-based sensors depend on their optical characteristics. CQDs based on xylan might be used as a dopamine (DA) sensor. Firstly, xylan compound was used as the stabilizing and reducing agent for synthesizing AgNPs and reducing graphene oxide (rGO) to give Ag@CQDs-rGO nanocomposite. Secondly, to make an electrochemical sensor, Ag@CQDs-rGO nanocomposite was placed onto a glassy carbon electrode [54]. Because of its potential utility in diagnostics, electrochemical sensing of DA is extremely important for understanding and simply treating neurochemical diseases. The linear range for monitor DA under perfect conditions was 0.1 to 300 μM, with a detection limit of 1.59 nM (S/N = 3). Finally, the suggested technique has the potential to widen the use of polysaccharide-based CQDs, and this sensor has the potential to provide a discriminative and accurate analytical platform for DA diagnostic techniques and drug evaluation.

Feng *et al.* [52] used the biopolymer xylan as a greener stabilizing and reducing agent dissolved in 2% NaOH aqueous solutions for producing extremely stable and evenly dispersed AuNPs. AuNPs were found to be well distributed, with diameters ranging from 10 to 30 nm, after thorough characterization. The ideal circumstance was as follows: the $HAuCl_4$ to xylan ratio was 1:10 (wt:wt) at temperature of 80°C, and the reaction duration was 40 min. The xylan/AuNPs composite showed extremely selective and sensitive cysteine sensing in aqueous solution, distinguishing cysteine from dozens of other amino acids, with a limit of detection of 0.57 M for cysteine. With the addition of xylan to the Au@Ag NPs, they demonstrated improved resistance to oxidation and corrosion of H_2O_2 [55]. Xylan molecules extracted from wheat bran (WB) were preserved AgNPs from oxidation and aggregation, which also formed hot spots in between NPs [56]. Harish *et al.* [57] extracted xylan from WB waste biomass to be used as AgNPs fabrication as following. Practically, prepared alkaline xylan solution by dissolved 25 mg of extract xylan powder in sodium hydroxide solution (49 mL of 0.2%). Then silver nitrate solution (1 mM) was added dropwise to the alkaline solution of xylan and heated at a temperature of 100°C for 30 min. The obtained of brown colour of solution indicated the silver reduction ion into AgNPs (size ranging from 20 to 45 nm).

Luo *et al.* [58] described a simple and environmentally friendly technique for producing extremely stable and evenly dispersed AgNPs using a polysaccharide of xylan as a stabilizing and reducing agent *via* the Tollens reagents of 20% ammonium hydroxides under MW. Due to the packing of xylan, the results indicated that AgNPs were well distributed with diameters of 20–35 nm. *In situ* reduction of AgNPs onto transparent bacterial cellulose papers have been carried out by Pourreza *et al.* [59]. In this method, cellulose nanofibres act as the reducing agent to produce an embedded AgNPs in a transparent sheet. According to the UV-Vis absorption spectra of the obtained AgNPs in cellulose sheet is to give very low absorbance in the pH of 6, but by increasing the pH values to 9.5, the broadening of UV-Vis absorption spectra values increased, indicating the better conversion of silver ions to AgNPs at pH 9.5. This due to the open end chains of aldehyde groups. Perez-Alvarez *et al.* [60] used poly(ethylenimine) to adjust the pH of cellulose solutions at basic

condition to produce CuNPs that were made using fibres of cotton as reducing agents in a green synthesis technique. The novelty here, the green synthesis technique, is low-cost and eco-friendly method, and it may be used on a bigger scale NP production.

3.2 Cellulose

Cellulose is a naturally biomaterial with 1, 4 β-glycosidic linkages in the structure and outstanding physicochemical characteristics, mechanical capabilities, and water absorption capability. These biodegradable fibrous structures are harmless, have a high crystallinity, and a huge surface area, and are chemically stable. They also garnered popularity as a result of its numerous applications in a number of different fields of study, including green synthesis of nanomaterials. Heidari and Karbalaee [61] used alkaline solution (pH = 12) of nanocrystalline cellulose without any other chemical agents to *in situ* green and eco-friendly synthesis of AgNPs at temperature of 65°C for 30 min. The obtained results showed that the shape of AgNPs of around 20 nm is spherical on the surface of nanocellulose (35–50 nm) and demonstrated catalytic efficiency towards the removal of 4-nitrophenol and methyl orange.

This environmentally friendly method, which allows for the creation of numerous shaped noble nanostructures without the use of toxic reducing agents such as hydroxylamine hydrochloride, $NaBH_4$, and so on, as well as a capping/surfactant agent, and which uses the benign biodegradable polymer CMC could have a wide range of technological and pharmacological applications. The reducing end groups of cellulose nanocrystals are modified by reductive amination to immobilize the gold ions. Under three different values of pH, the reducing groups were chemically modified through reductive amination using sodium cyanoborohydride (Cn) and sodium triacetoxyborohydride (Ac) or 2-picoline-borane complex (Pc). The pH of the reaction medium was discovered to be a critical factor in the green synthesis effectiveness of reduction reactions. The amine group of the molecule is deprotonated at pH 9.2, allowing the reductive amination process to be more efficient. Because the thiol concentrations obtained with the reducing agents Ac and Pc were similar to those obtained with Cn at basic pH. It can be confirmed that at pH 9.2, which corresponds to the amine's pK_a, all three reducing agents produced the maximum conversion [62]. As a result, topochemical reactions may be used to attack reducing end-groups in open-chain aldehyde forms, allowing for end-wise alteration of original cellulose molecules. The open-chain aldehyde is achieved in alkaline media or by another's chemical modifications reactions of cellulose such as reactions of cellulose end aldehyde groups with 9*H*-fluoren-2-yl-diazomethane [63], n-conjugation of aldehydes with 4-amino-3-hydrazino-5-mercapto1,2,4-triazole [64], e carbazole-9-carbonyloxyamine [65], hydroxylamine hydrochloride [66], and sodium chlorite [67]. Compared to another reduction reactions the use of cellulosic compounds as reducing agent of ions in alkaline conditions is ecofriendly due to it has the advanced of easy process, low price and renewability.

4 Solvents of green reaction

The appropriated catalyst-assisted reactions and the right choice of solvent are two essential elements of green methods in organic chemistry. Aromatic halogenated solvents should not be utilized as they are volatile, poisonous, and deplete the ozone layer. Ionic liquid (IL) can be utilized as an alternative as they are non-volatile, non-aqueous, and polar. If an organic reaction allows for product separation by condensation or extraction, the catalyst may stay in the solvent; in this instance, both the catalyst and the solvent can be used again. Organic processes can also be performed there without solvents in a SC medium of CO_2 (one alternative is MW.

Solvents are expected to account for more than 80% of the reaction mixture used in the production of NPs. The sensible selection of solvents has become a fundamental precondition for the design of green chemical manufacture due to their high impact on the environment. Solvents are frequently used in the synthesis of NPs as a medium for dissolving precursors, transporting heat and reactants, and distributing the resultant NPs. The green synthesis processes heavily avoids the usage of organic solvents with significant toxicity despite the fact that careful safeguards are available in laboratory research. Water is environmentally friendly as it is harmless and nonflammable, and it is economically accessible owing to its cheap cost and plentiful supplies. Water has the largest heat capacity of any substance, and the high energy inputs associated with water-based production make it difficult to meet the need for energy-efficient production. Over the last decade, a lot of studies have focused on finding solvent alternatives to alleviate the environmental concerns SC fluids such as SC carbon dioxide (CO_2), and ILs are all good examples. Ordinary solvents become SC fluids at temperatures over the critical temperature, which have significantly more free space and are more compressible. A number of basic

physical characteristics, such as density, diffusion coefficients, and thermal conductivity, are dramatically altered in the SC state. Importantly, these characteristics may be switched between "gas-like" and "liquid-like" states with a simple change in pressure and/or temperature, providing the foundation for novel synthesis methods that use SC fluids as solvents. The dielectric constant varies significantly near the SC point in the SC state. As a result, SC hydrothermal production of NPs can be controlled by adjusting the dielectric constant and is more eco-friendly because it just uses water as a solvent (the critical temperature is 646 K and pressure is 22.1 MPa).

At pressure and temperature over the critical point, solvents could be transformed into SC fluids. Solvent characteristics such as viscosity, heat capacity, and density are drastically changed in the SC state. In addition, water may be used as a SC solvent in a variety of green processes, it has a critical pressure of 22.1 MPa and a critical temperature of 646 K [68]. CO_2 has been the most practicable, non-hazardous, and harmless SC fluid [69,70]. AgNPs and CuNPs can be synthesized in SC CO_2 [71]. Sue *et al.* proposed that diminishing the solubility of metal oxide towards the critical point might lead to super saturation and the eventual NPs creation [72]. Kim *et al.* used sub-critical and SC water and methanol to create NPs of tungsten oxide and tungsten blue oxide [73].

SC hydrothermal methods help to create a greener environment by using water rather than an organic solvent to create a variety of useful materials that help to reduce CO_2 emissions. Furthermore, because the processes are very rapid, SC hydrothermal techniques can treat many more reactants and products than traditional methods. As a result, we feel that commercializing such methods makes a significant contribution to a greener environment. The SC hydrothermal NP synthesis of metal oxide is environmentally friendly not only because it uses just water as a solvent but also because the NPs produced help to create a more sustainable environment. For example, Xu *et al.* [74] investigated the impacts of temperature, water flow rate, and concentration of reactant on the particles morphology and size of lithium iron phosphate ($LiFePO_4$) NPs by continuous and batch hydrothermal synthesis. In general, the continuous hydrothermal approach produced smaller sized NPs with a regular structure, whereas the batch method produced micron-sized particles and much less uniform. Particle size and size distribution improved with temperature in the continuous technique, whereas the converse was true in the batch method. In the continuous technique, particle size grew with reactant concentration, whereas in the batch method, particle size declined with reactant concentration. In general, particle size increased with increasing reactant concentration and temperature. However, $LiFePO_4$ NP morphology became more regular at high water flow-rates due to better mixing characteristics. This implies that the relative nucleation rates of particle and growth in the two approaches are significantly different. Sue *et al.* [72] showed that the solubility of materials was substantially influenced by the dielectric constant change. The solubility of metal oxide reduced towards SC point, approaching supersaturation, resulting in the harvesting of a significant number of nuclei and the production of small-sized NPs. As a result, SC hydrothermal synthesis for the creation of NPs with a restricted size distribution is theoretically possible. Organic molecules were added into the SC hydrothermal synthesis to improve the dispersibility of as-synthesized NPs in various solvents for diverse applications [75]. IL (liquid state at temperature of ≤100°C) is constructed from ions, ion pairs, and ionic compounds, and it is the best solvent after water for NPs green synthesis; it is indeed salt usually at room temperature. IL examples may be of cationic composition such as 1-alkyl-3-methylimidazoium, *N*-alkylpyridinium, PR_4^+, NR_4^+ or anions composition such as tosylate, alkylsulfate, $[PF_6]^-$, $[BF_4^-]$, $[CH_3COO^-]$, Cl^-, NO_3^-, and $[CF_3SO_3^-]$. In comparison to conventional ionic compounds, IL molecules have a much poorer symmetry. In contrast to water, where water molecules are chemically H-bonded, and organic solvents, where molecules of organic are bonded together by van der Waals interactions, Coulomb interactions are the dominant interactions in IL. Usually, IL solvents are having thermally stable, electrically conducting, viscous, and low vapour pressure (~10 Pa at ambient temperature); some of them have magnetic property such as 1-butyl-3-methylimidazolium tetrachloroferrate. Chemical compounds' solubility in ILs is controlled by H-bonding and polarity of compounds. ILs are utilized for a variety of applications, including gas treatment, coal manufacturing, pharmaceutical manufacture, nuclear fuel reprocessing, and cellulosic handling. "Room temperature ionic liquids" is another name for ILs. In ILs, several metal NPs (*e.g.* Al, Te, Au, Ag, Ru, Pt, and Ir) have been green synthesized [76–79]. Because the IL may act as both a reductant and a stabilizing agent, the NP green manufacturing process can be easily done. ILs can be have hydrophobic or hydrophilic properties depending on the nature of anions and cations. For example, tetrafluoroborate (BF4) analogue is hydrophilic, whereas 1-butyl-3-methyl imidazolium (Bmim) hexafluorophosphate (PF6) is hydrophobic, Since both molecules are ionic, they can act as catalysts for several reactions includes ionic polymerization reactions [80–83]. Bussamara *et al.* [84] used imidazolium and oleylamine as IL and a conventional solvent, respectively

in a comparative study to control the manganese oxide (Mn_3O_4) NP production. They observed that in ILs, manganese oxide (Mn_3O_4) NPs (9.9 nm) have smaller size produced than in the oleylamine solvent (12.1 nm). Lazarus *et al.* used IL of (BmimBF4) to synthesize isotropic spherical and large-sized anisotropic hexagonal structure of AgNPs [85]. In mild conditions, IL was utilized as a replacement for water in the electrolytic process, and this was important in an electrochemical technique [86]. Kim *et al.* used thiol-functionalized ILs (TFILs) for one-phase green preparation process for NPs of platinum (Pt) and gold (Au), where TFILs acted as a stabilizing and reducing agent [87]. Dupont *et al.* used IL of 1-*n*-butyl-3-methylimidazolium PF6 act as a reducing agent at ambient temperature for synthesizing NPs of Ir (2 nm). Surprisingly, the IL medium is ideal for creating reusable biphasic hydrogenation catalytic systems [88].

The following are some of the advantages of utilizing ILs rather than conventional solvents: (1) in order to support biocatalysts, several metallic catalysts, polar organic molecules, and gases can be readily dissolved in ILs; (2) ILs have positive thermal stabilities, allowing them to operate across a wide temperature range. Most of them melt at ambient temperature and start to degrade at temperatures of 300 to 400°C. As a result, they have a much wider synthesis maximum temperature (two to five times) than water; (3) the cations and anions coupled with IL can be modified to alter its solubility characteristics; (4) ILs are non-coordinating unlike other solvents such as esters and alcohol; and (5) because ILs have low vapour pressure, they do not escape into the atmosphere like an organic solvent. Because they include both anions and cations moieties, ILs have dual functions. ILs are not suitable for the creation of metallic NPs in biomedical applications because of their non-biodegradability issues. Many novel researchers have established biodegradation ILs with an optimum efficiency [89–92].

5 Synthetic promising green routes using gamma irradiation

Radiation generated by radioactive atoms or reactor sources, such as γ rays and X-rays, or particle energy, such as electron beam radiation is referred to as irradiation technique. Such particles, also known as photons, are known to have enough energy to break or initiate chemical bonds, as well as to produce electrically charged species when they contact with atoms or molecules. The use of γ rays has been recognized as a valuable method for the creation and synthesis of NPs among other conventional methods including harmful catalyst and solvents. In principle, the utilizing radiation to make NPs involves the radiolysis of solvent, and the useless of a reducing agents, in which a solvent molecule is ionized and excited, resulting in the production of a range of reactive species, which subsequently drives the synthesis of NPs.

Particularly, gamma-rays having smallest wavelengths and high energies (1.17 and 1.33 MeV from ^{60}Co) can be used in the green synthesis approach of NPs [93–102]. Gamma irradiation is an eco-friendly method, high penetrated, non-selective, and fit to several cases of reactions (solids, liquids, or gases). The green approaches of gamma irradiation arise from water radiolysis. The reactive six species hydrated electron (e_{hy},) pair atom radicals ($H^{\cdot}$ and $^{\cdot}OH$), hydronium ions H_3O^+ and pair molecules (dihydrogen H_2 and hydrogen peroxide H_2O_2) that are results from water radiolysis. Hydrated electrons (e_{hy},) and ($H^{\cdot}$) hydrogen atoms are strong reducing agents with standard potentials $E°(H_2O/e_{hy}) = -2.9\ V_{NHE}$ and $E°(H^+/H^{\cdot}) = -2.3\ V_{NHE}$. In contrast, hydroxyl radical ($^{\cdot}OH$) is a strong oxidizing agent with a standard potential $E°(HO^{\cdot}/H_2O) = +2.7\ V_{NHE}$ [103]. And hydrogen peroxide H_2O_2 has two standard potentials depending on the pH of the reaction [104–106]:

$$H_2O_2 \rightarrow O_2 + 2H^+ + 2e^-, \quad E^o = -0.682\ V_{NHE}, \quad (1)$$

$$H_2O_2 \rightarrow 2H^+ + 2e^- \rightarrow 2H_2O, \quad E^o = +1.776\ V_{NHE}, \quad (2)$$

From above it is clear that the reduction–oxidation reaction takes place at the same time, and this means that when metal procurer is dissolved in water exposed to gamma irradiation, it will undergo reduction or oxidation reaction according to their standard potential values. Dissolved metal ions can be oxidized (*via* molecule their redox potentials are greater than the metal ions) or reduced, depending on the standard reduction potential of the dissolved metal ions (*via* molecule their redox potential is lower than that of the metal ions). For example, under gamma irradiation, the copper ion solution undergoes reduction to give CuNPs [107,108]; in contrast, the iron and cobalt undergo oxidation reaction [109] [110]. The redox potential of Fe^{2+}/Fe^{3+} is 0.77 V_{NHE}, and the soluble Fe^{2+} can, therefore, be easily oxidized to insoluble Fe^{3+} by any species of the powerful oxidizing agents, $^{\cdot}OH$ as well as by less powerful oxidizing agent H_2O_2 ($(H_2O_2 + 2H^+)/2H_2O$) $E = +1.763\ V_{NHE}$). For cobalt, the redox potential of Co^{2+}/Co^{3+} is 1.81 V_{NHE} and therefore radiolytic oxidation of dissolved Co^{2+} to less soluble Co^{3+} oxides/hydroxides requires the more powerful oxidizing agent $^{\cdot}OH$. In attention, under continuous gamma irradiation and water radiolysis both oxidizing as well as reducing

species are generated in the same manner. The (e_{hy},) and (H˙) are responsible for the nucleation of NPs, but the presence of ˙OH, if not sufficiently scavenged, may have the opposite effect due to its highly oxidising characteristics, which may counteract the reductions. If ˙OH radicals are properly scavenged, they could improve the reduction reaction, which will enhanced the nucleation process of dissolved metal ions. The progress of reduction-oxidation reactions is directly dependent on the temperature and pH of the reaction media, initial concentration of dissolved metal ions, and scavengers kind. If we want domain ions reduction reactions to take place, the oxidizing radical scavenger should be added such as diethylene glycol [111], isopropyl alcohol [112], and polyvinyl pyrrolidone (PVP). Moreover, if we want to domain ions oxidation reactions to take place, the reducing radical scavenger should be added such as nitrous oxide N_2O and *t*-butanol or O_2 [113]. As a result, the method of NP creation by a continuous radiation source without any scavenging of oxidizing or reducing molecules would be completely different.

In addition, the creation of a cluster of regulated NPs in aqueous conditions, following nucleation, is not stable as the aggregation process tends to continue until high nuclearity values are attained, resulting in precipitation of NPs. As a result, a suitable stabilizer, such as a polymer and/or surfactants as stabilizing agents, is required to prevent or stop the aggregation process, resulting in the cessation of coalescence, whether due to electrostatic repulsion. This technique is divided into two parts: the first involves contacting the support with an NP solution and the second involves directly irradiating the supporting matrix in contact with the metal ion solution after the precursors have been adsorbed onto the support. In the last method, the supporting matrix must have a specific amount of hydrophilicity as well as chemical groups, such as carboxylic, amine, and hydroxyl, among others, that allow metal ions to be adsorbed *via* chelation or electrostatic interactions, resulting in desired synergies. By chemically stabilizing nanocrystals, passivating compounds can reduce the polydispersity of NPs; that is, thiol-containing ligands and the varying of the capping agents quantity, such as polymers, that is, PVP or surfactant molecules with surface-active functional groups could change the form and size of the resulting NPs [114]. As a consequence, the reduction of polydispersity with the usage of stabilizing agents is an influence on the NP size and NP morphology *via* those compounds. For instance, with the polymer as a capping agent, the size of the product decreases as the polymer content in the synthesis medium increases. This might be because an increased polymer concentration in the solution decreased the mobility of metal ions, preventing the aggregation of NPs into larger sizes.

For example, the production of CuNPs on grafted membranes with poly(acrylic acid), in which the reduction reaction of Cu^+ ions take place by gamma irradiation when using ethyl alcohol as a scavenger [115]. The obtained CuNPs is colloidal due to their total energy potential of an interaction between the two NPs is high. The total energy potential of an interaction between the two NPs, according to the Derjaguin–Landau–Verwey–Overbeek theory, is the sum of attracting (van der Waals) and electrostatic repulsion (coming from the double layer of electric charges). The particle is deemed stable if its total energy potential exceeds the kinetic energy of its motion. The stability or instability of NPs cannot be represented just by electrostatic stabilization; the surface energy must also be considered, as previously mentioned. Substantially, different metals ions have a surface energy ranging from 1,000 to 2,000 mJ m^{-2}, which is greater than that of other inorganic and organic compounds, which have energies of less than 500 mJ m^{-2}; these metals with high surface energy, combined with others *via* dipole–dipole interactions, contributes to the instability of nanomaterials [116]. The repulsion among molecules or ions deposited on nearby particles is known as steric stabilization. The larger the adsorbed particles, the more effective they are in stabilizing NPs due to geometric constraint. The spatial shape of the molecules is also crucial because elongated or conical conformations have been shown to aid stability. Therefore passivation and encapsulation occurs when the NP size is less than the length of the stabilized agent. Generally, stabilized agent should contain chemical groups with an electron pair, such as (P, S, O, and N) moieties, or unsaturated aromatic molecules have π electrons, they strongly adsorb on surfaces of the metal NPs [117]. Phu *et al.* [118] used of chitosan as a stabilizer and radical scavenger in the gamma irradiation production of AgNPs (Ag/NPs-10 nm) at dose of 8–40 kGy. Based on the UV-Vis spectroscopic analysis, the rise in chitosan concentration from 0.5 to 1.0% reduced the size of silver particles from 11.3 nm to around 7.0 nm. Li *et al.* [119] used two different methods, conventional chemical reduction by 1% sodium citrate and gamma-irradiation-based reduction at dose of 40 kGy to prepare gold and silver NPs from their respective salt solutions at various ($AgNO_3$: 2×10^{-4} to 2×10^{-2} M; $HAuCl_4$: 2×10^{-4} to 2×10^{-3} M) concentrations. In radiation approach, PVP and 2-propanol were used as a stabilizer agent and radical scavenger, respectively. Sodium citrate was widely used as a reducing agent and as stabilizer in several NP synthesis. Based on TEM images to compare the two NPs (Ag and Au), in terms

of concentrations, the two procedures provided distinct results. In comparison to traditional chemical reduction procedures for generating highly concentrated silver and gold colloidal particles with smaller sized dispersion, the gamma-irradiation-based strategy has made great progress. Vo *et al.* [120] compared between electron beam and gamma irradiations for the synthesis of AuNPs from a stock of 10 mM HAuCl4 solution. Chitosan molecules are used as a stabilizer. The author studied the irradiation dose effect and concentration of chitosan. UV-Vis spectrophotometric features indicated that the smaller NPs are formed at high doses is correlated with the extent of chitosan scission chain. This explain why the concentration of chitosan is not sufficient to prevent NPs aggregation. In addition, in a continuous water radiolysis as induced by gamma-irradiation, the gold ions association with their NPs (gold) clusters is faster than the reducing species generation, which grow as clusters by the reduction of gold ions. However, in the high doses of e-beam and gamma irradiation, all reducing species are formed and scavenged in a short time, followed by the generated stages of AuNP individually. In the case of radiation synthesis of NPs, a variety of settings and parameters may be tuned to regulate the nucleation process, which has a direct impact on NP properties such as solvent, gamma irradiation doses, pH, temperature, and precursor concentration.

5.1 Solvent

The interaction between atoms and solvent is dependent on the dielectric constant and polarity of the solvent and appears to have a crucial impact. Constantly, an extra solvent is associated with the atoms are produced in a uniform manner due to the atom-solvent bond energy.

The solvent dependence of absorption spectra in solutions is proof of the substantial effect of the atom-solvent interaction. For example, the wavelength maxima is blue-shifted of the UV-Vis spectroscopy of Ago and Ag^{2+} with the increasing polarity of solvent and dielectric constant [121,122]. In addition, the existence of reducing agents in the solvent has the greatest impact on particle size and dispersion; so the faster the reduction reaction, the smaller the particles obtained.

Here, the irradiated solvent is itself the reducing agent; for example, water but the $^{\cdot}OH$ radicals are strong oxidants, and should be avoided. They can be scavenged by adding a scavenger molecule of $^{\cdot}OH$ radicals, such as *t*-butanol and primary alcohol or secondary alcohol or formate ions, which produce high yield solvated electrons (e_{hy}) and $H^{\cdot}$ radical, that are powerful reducing agents at ambient temperature.

Practically, the use of alcohols as solvents has strong reducing properties due to the solvated electrons, and $^{\cdot}H$ atoms are produced primary after irradiation process. The reducing radiolytic species yield is less in low dielectric solvents such as THF or propylene glycol monomethyl ether acetate than in more polar solvents. The radiolysis of these solvents will yield cation species on the solvent + molecules that partially recombine with the hydrated electron (e_{hy}). At a certain irradiation dose, these solvents may produce and grow up stable AgNPs and AuNPs due to a positive charge repulsion.

It concluded that the irradiated solvent could be used as a reducing agent, and a reducing chemical is unnecessary. For example, Balcerzyk *et al.* [123] used irradiated aqueous acidic and neutral silver ions solutions to study the dynamics of the silver reduction in both solutions. Ten solutions of silver ion concentrations (10–150 mM) were subjected to picosecond pulse radiolysis experiments (pulse width 7 ps). The studies were conducted out in a neutral water solution and a strongly acidic phosphoric acid solution. The pump probe method was used to evaluate the AgNPs yield inside the electron pulse at varied concentrations of silver ions by measuring both the decay of the hydrated electron (e_{hy}) and the formation of AgNPs. The obtained results showed that at low concentration of silver ions (0.1 up to 0.8) mol L^{-1}, the AgNPs yield is high from acidic solutions than neutral solutions at the end of a 7-ps pulse. However, at high concentration of silver ions (0.12 and 0.15) mol L^{-1}, the AgNPs yield is high from acidic solutions than neutral solutions at end of a 7-ps pulse. This might be due to two reasons: (1) the formation of ion pair between the hydrated electron (e_{hy}) and H_3O^+ and (2) the viscosity of phosphoric acid at high concentration of silver ions solutions ((0.12 and 0.15) mol L^{-1}) restricts the motion of hydrated electron (e_{hy}) for nanoseconds compared to neutral solutions.

Dey *et al.* [124] used irradiated 2-propanol solvent (dose rate 1.8 kGy h^{-1}) that displays strong reducing species of e_{hy} and $(CH_3)_2C^{\cdot}OH$ (2-hydroxyl-2-propyl radical) to take an active function in gold ion reduction. Finally, solvent radiolysis typically have a crucial responsibility in the NP synthesis.

5.2 pH

The NP size appears to be influenced by the pH, as the SPR band from the NPs tends to red-shift as the pH rises, accompanied by a loss in stability and a higher

inclination to agglomerate. Ghobashy *et al.* studied the effect of pH (1, 5, 8, and 13) in terms of size and nanostructure of poly aniline (PAni) in DMF solvent. UV-visible spectroscopy revealed that the smallest particles of PAni NPs can easily be obtained at low pH.

The TEM images revealed that the nanopolyaniline prepared at pH 1 and pH 5 is nanosphere of 5 nm. Also, the nanopolyaniline yield is higher at pH 1 than at pH 5, which can be attributed to the electrostatic interaction among the end sites of the chloride atom in the PAni chain at pH 1. However, due to the aniline polymerization of at both pH 8 and pH 13, the polyaniline NP formation are in a rod-shaped structure, which becomes bimodal structure by the existence of both oligomeric and polymeric polyanilines [125]. Liu *et al.* [126] founded that copper ions solution could be oxidized when the pH of solution lower than 9. Ramnani *et al.* observed that the size of Ag nanoclusters was increased with increasing pH of the irradiated solution [127].

5.3 The radiation dose

Another element that influences the development rate and size of NPs is the radiation dose, which is particularly noticeable in the case of NPs. It has been shown that for low radiation doses, the resulting low reducing rate results in a fewer number of metal nuclei than metal ions.

Processes of aggregation and nucleation in the NP formation could be affected by the absorbed dose. The growth rates could be determined by probabilities of the atom collisions [128]. At low radiation dose, the unreduced ions of higher than the concentration of nucleus due to a low yield of reduction reactive species. However, at higher radiation doses, most of the dissolved ions are consumed during the nucleation and reduction process; therefore, the concentration of atom nucleus is higher than the unreduced ions concentration. As a result, at higher radiation doses, the NPs are smaller in size. Rau *et al.* [129] synthesized AgNPs using different gamma irradiation doses in the presence of gum acacia as a stabilizing agent. It was found that according to the UV-Vis spectroscopy as the irradiation dose increases, the intensity of AgNPs optical absorption increases with blue shifts, and this means the amount and size of AgNPs increased, respectively. It concluded that, the shape of final NP products is influenced by the reduction rate and growth of NPs during the radiolytic production of solvent, which may be influenced by changing the irradiation doses. For example, during the radiation synthesis of AgNPs at low irradiation dose (30 kGy) of gamma irradiation in the existence of PVA, when the initial rate of growth is slow, the PVA capping agent takes over, resulting in the formation of small spherical AgNP (Figure 6). By increasing the dose of gamma irradiation (100 kGy), rapid adsorption of the cross-linked chains of PVA on the face of AgNPs result in the creation of triangular nanoplates from spherical nanoplates [130].

6 Bio-inspired green nanotechnology for energy efficient materials

The implementation of green nanotechnology as an effective replacement for conventional nanotechnology, addressing environmental issues, should be performed in a way that incorporates the concepts of green science, that is, by developing nanomaterials and goods without harming the environment or human health, using the lowest possible energy costs, and creating the lowest possible waste/pollution. To discuss the applications of nanoscale membranes, nanocatalysts, and nanosensors in various areas of science and

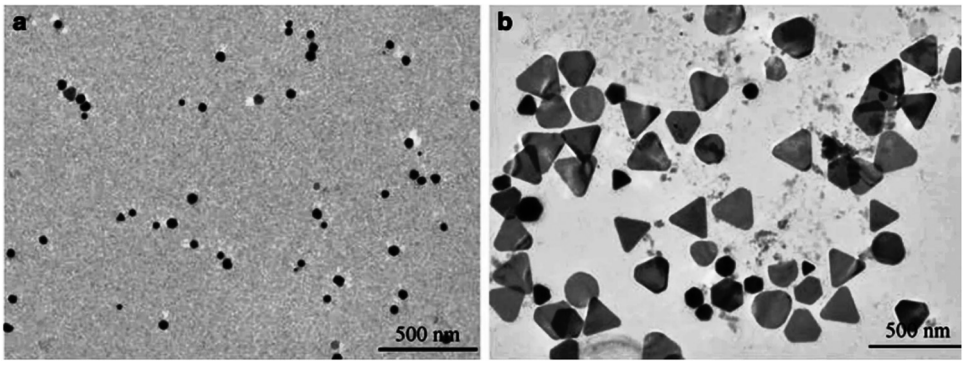

Figure 6: TEM pictures of irradiated Ag colloids samples at various gamma doses: (a) At 30 kGy, the majority of the resulting particles are spherical and (b) triangular nanoplates dominate at 100 kGy [130]. Copyright 2016.

technology is fitting here. In addition to safe use of plant-derived NPs, modifying herbal therapies using nanostructures can improve the dissolution and bioavailability of poorly soluble drugs as well as decrease their toxicity [131–134].

Biosynthesized NPs offer significant benefits, such as treatment and diagnosis of various diseases, and contribute to future generations of therapies as building blocks. Phyto synthesized nanostructures are now among the most useful NPs as they demonstrate multiple applications in various aspects of human life, such as health care, food and feed, cosmetics, and biomedical science. Many advantages of using plant sources to biosynthesize NPs include their cost-effectiveness, green and sustainable methodologies, flexibility, and versatility, in addition to these applications. Plant oil compounds have recently become viable for biocompatible NPs to be biosynthesized. In many cases, biomolecules that originate from biological organisms are used to control NP nucleation and development. The antimicrobial potential of critical oil-based NPs can, therefore, exert synergistic antimicrobial effects, which represent a new approach to this challenge [134]. Green chemistry methods used for synthesizing metal oxides nickel ferrite ($NiFe_2O_4$) NP-mediated plant extract from Persa-Americano seeds [135]. Ramanarayanan *et al.* [136] incorporated bio-inspired AgNPs into the titanium dioxide (TiO_2) NPs photoanode solar cell. The obtained results showed that the photoanode solar cell of Ag-TiO_2 an improved efficiency of Förster resonance energy transfer 6.69% as compared to blank TiO_2 photoanode 4.85%.

Inspired by nature, researchers in several studies have demonstrated a synthetic strategy to stabilize bio-inspired nanomaterials. Their findings are a significant breakthrough in functionalizing molecular assemblies for future technologies. Despite severe changes in temperature (heat or cold), practically photosynthetic organisms may be found in every part of the earth, attempting to harvest sun energy. Uncovering nature's secrets for effectively and reliably harvesting light might change the landscape of green sustainable solar energy technology, especially in the face of rising global temperatures. The interaction between light and supramolecular assemblies is the initial stage in photosynthesis (light harvesting). Nature devised a two-component system in which supramolecular assemblies are anchored within protein or lipid scaffolding in everything from leafy green plants to microscopic microorganisms. To simulate and match scaffolding of protein in photosynthetic organisms, Ng *et al.* [137] synthesized the cage-like scaffold to stabilize the entire supramolecular structure of light-harvesting nanotubes (LHNTs) has a size of ~5 nm with cross-linking molecular silanes: (3-aminopropyl)trimethoxysilane and tetraethyl orthosilicate. The obtained results confirmed the high structural stability of (LHNTs) under environmental stress.

An effective organic photoelectrochemical cell is built using chlorophyll*a* (Chll*a*) and NPs of silver and gold have been studied in several literatures. For example, in a water-based dye-sensitized solar cell (DSSC) Lai *et al.* [138] used the aqueous $Ce^{4+/3+}$ electrolyte system, and AuNPs (6 nm) were used as a Schottky barrier on the substrate of TiO_2 as electrode loaded with natural alcohol extracts dye from *Garcinia subelliptica*, *Bougainvillea brasiliensis* Raeusch, *Ficus Retusa* Linn. and *Rhoeo spathacea* (Sw.) Stearn in comparison of the commercial dyes such as chlorophyll, crystal violet, and mercurochrome. The obtained results showed that the extracted dye from *R. spathacea* (Sw.) Stearn gives 1.49% of the solar conversion efficiency.

Fruits, flowers, leaves, bacteria, and other naturally occurring items come in a variety of colours and contain a variety of dyes that may be easily extracted and used in DSSC. These natural dyes used as photosensitizers in DSSC due to their substantial absorption coefficients in the visible region, relative abundance, simplicity of extract, and environmental safe.

Barazzouk *et al.* [139] studied the interactions of excited-state between AuNPs and Chll*a*. The obtained results showed that the Chll*a* emission intensity is quenched after doped AuNPs. This due to the photoinduced electron-transfer process from excited state of Chll*a* to AuNPs. Due to this overlap and interactions between fluorescence of Chll*a* and AuNPs, the energy-transfer process can take place. A photoelectrochemical cell based on Chll*a* and AuNPs is created using these features of AuNPs. The advantageous effect of AuNPs in accepting and shuttling the photogenerated electrons in Chll*a* to the collecting electrode, resulting in an increase in charge separation efficiency, which explains why this cell with AuNPs outperforms others without the AuNPs. Calogero *et al.* [140] manufactured DSSCs-based TiO_2 NPs films and natural dye extracted by immersed red turnip and bougainvillea flowers' leaves in HCl solution (0.1 M). The best results of solar energy conversion efficiency with the red turnip extract was 1.7%.

In general, all environmentally friendly inventions that involve energy efficiency, recycling, health and safety concerns, renewable resources, *etc.* fall under the umbrella of green technology. Thermal disks and solar panels are good examples of innovations in the fields of energy conservation and electricity generation that use renewable heat from the sun to produce electrical energy in a healthy and environmentally friendly way. Sustainable and green chemicals such as detergents, cleaning agents, and insecticides can be made using environmentally safe and green reagents

such as coconut, glycerin, orange, and peppermint oil, avoiding the use of any toxic or hazardous materials. Green technology makes use of recycled and recyclable materials and solar charging systems when producing different products. The creation of green science and technology, therefore, provides comfort, makes economic sense, and offers a safe and sustainable living environment [12].

7 The role of ascorbic acid in NPs green productions

Ascorbic acid is a multipurpose compound that has been revealed to have the capacity to operate as a NP stabilizing and reducing agent. However, for certain NPs, such as CuNPs, ascorbic acid is a poor stabilizing or reducing agent by itself [141]. CuNPs are often produced using inert gases such as nitrogen and argon because some NPs can oxidize quickly in air or aqueous conditions. However, because of the antioxidant qualities of ascorbic acid, it might be used to prevent the further oxidation of the CuNPs synthesis. Ascorbic acid has a potential energy of +0.08 V; so with a typical reduction potential greater than 0 V of metal ions, such as Cu^{2+}, Ag^{+}, Au^{3+}, and Pt^{4+}, can be easily reduced, but ascorbic acid cannot reduce metal ions and have reduction potential less than 0 V such as Fe^{2+}, Co^{2+}, and Ni^{2+}. Ascorbic acid can release hydrogen that rapidly react with dissolved ions and reduce them. Because ascorbic acid has a large number of hydroxyl groups, it is used in certain investigations to combine the effects of reduction reactions with other green substrates that have a poor capacity to convert copper ions to CuNPs. Ascorbic acid at larger concentrations might be more powerful as a stabilizing and reducing agent. Chemically reduction process of copper ions salts by L-ascorbic acid is a novel and environmentally friendly method in different green synthesis methods in which L-ascorbic acid, VC, that is an excellent oxygen scavenger, behaves as both a reducing agent and stabilizing agent to effectively reduce the metallic ions precursor and inhibit the common oxidation reaction of newly formed pure copper nanocrystals.

Wang *et al.* [142] fabricated copper nanocubes using the solution-phase reduction technique with ascorbic acid used as a reducer and PVP used as the capping agent (Figure 7). The addition of PVP to the reaction system may have accelerated growth in the [001] direction while slowing growth in the [111] direction of CuNPs.

8 Potential application of NPs green synthesized

The number of scientific publications in the subject of nanotechnology has increased in the recent decade. Green nanomaterials play an important role in the use of nanotechnology in a variety of sectors. Green nanotechnology is the creation of green nanoproducts and their use to achieve long-term sustainability.

8.1 Solar cell

Solar conversion systems have been seen as a promising way of meeting the increasing interest for vitality among the different sustainable power sources. Three generation technologies for solar production were considered when manufacturing the first solar cell. The first-generation and second-generation solar cells depended on Si

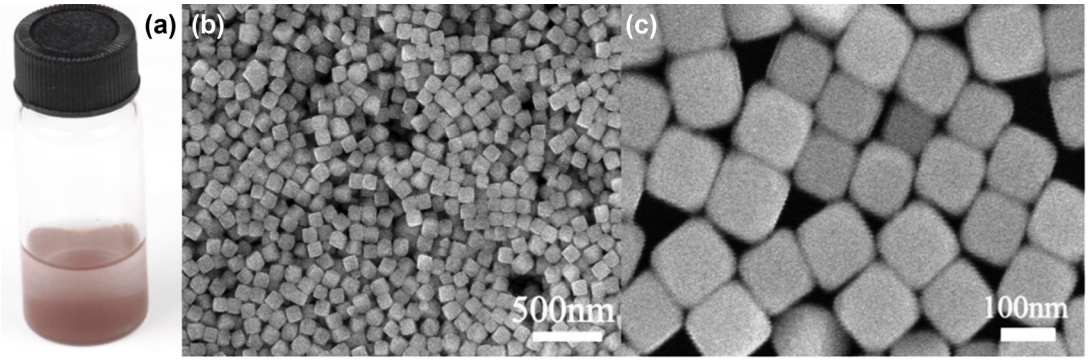

Figure 7: Figure 7 show the (a) colloidal solution of copper nanocubes and the TEM images (b–c) of well-defined copper nanocubes using the solution-phase reduction technique with ascorbic acid is used as a reducer and PVP as the capping agent [142]. Copyright 2006.

nanocrystalline wafers and composed, respectively, of thick (200–300 μm) and thin (1–20 μm) semiconductor films. As the cost of production in first-generation and second-generation solar cells is high, solar cells of the third generation were built. The concept for designing solar cells of the third generation was to reduce costs while increasing the energy conversion efficiency.

DSSCs have recently gained the attention of researchers as one type of third generation solar cells [143]. As another type of third-generation solar cells, quantum dot sensitized solar cells (QDSSC) is one of the most promising, cost-effective, and an alternative to conventional silicon cells due to its distinctive features [144]. Theoretical calculations show that QDSSCs can surpass efficiency by up to 44% due to multiple exciton generation effect. However, quantum dots in nanosized have more benefits such as high coefficient of extinction, size-dependent properties, low cost material, easy processing, and photo stability. Most of materials utilized in sun powered cells sharpened to QDs depends on cadmium nanoparticles or other harmful materials, for example, lead nanoparticles (PbNPs) and tin nanoparticles. Recently, Cd-free and low-toxic nanocrystal of $CuInS_2$ single core was utilized as an option in contrast to harmful QDs in QDSSCs [145]. The CuZnSnS solar cell based on nanocrystal has recently been introduced as another Cd-free and eco-friendly solar cell. The efficiency of solar cell has been improved by using the light sintering technique [146].

Zavaraki *et al.* [147] used novel Cd-free and low toxic colloidal binary InP and ZnP quantum dots passivated with ZnS nanocrystal as another option for potential environmentally safe QDSSCs. Such QDs were synthesized under the flow of nitrogen using hot injection technique to prevent contamination with oxygen. It is observed that ZnS-passivated InP shows down-shift in the energy from the band gap, which is responsible for wider absorption. Higher power conversion performance of InPZnS QDSSCs is due to wider absorption range and higher electron injection efficiency compared to that of single core InP NPs. Under light illumination, photogenerated electron is directly injected into the TiO_2 substrate conductive band, as the thickness of the ZnS shell is designed to be as thin as possible to allow the injected electron to TiO_2 NPs. Photogenerated hole is transferred to electrolyte to allow the reset of QDs. In quantum dot-sensitized solar cells, Green Cd-free colloidal InP and ZnS-coated InP QDs have been successfully used as sensitizers. In QDSSCS, this was to provide an alternative to highly toxic QDs dependent on Cd, Pb, and Hg. ZnS-coating was found to not only induce red-shift in the onset of absorption of InP QDs but also protect InP against moisture and electrolyte.

The compounds containing the azo groups have been commonly used in the dye-sensitive solar cell, but the use of these polymers in single-layer polymer solar cells (PSCs) is not researched. Nevertheless, azo-associated polymers can potentially result in strongly light-absorbing chromophores appropriate for use in PSCs. This possesses the ability to be used in different areas such as solar cells and sensors because of the shape, morphology, and conductivity of the synthesized polymer. The PSC was manufactured with FTO/TiO_2/PPAAB/Al structure by poly(*p*-aminoazobenzene) PPAAB, and the efficacy of PPAAB on the efficiency of the solar cell was investigated [148]. The polymer exhibited strong thermal stability, semi-conductive compound conductivity, and nanosheet morphology. This polymer also has a fairly high power conversion efficiency and a relatively high visible area absorption in the solar cell from 300 to 800 nm due to its nanosheet structure and an strong contact surface between the chains [148–150]. The $[Ru(bpy)_3]^{3+/2+}$ species currently the most common dye used in DSSCs. The photo-produced electrons can, therefore, restrict the movement of the produced Ru^{II} and the resulting holes in the valenus after Ru^{II} excitation in its LMCT (ligand-to-metal charge transfer) band. However, when dealing with Boron-doped diamond (BDD), the ruthenium dyes are not the right ones for sensitization. One potential explanation may be because of the Ru-complex HOMO's too low position compared to BDD's valence band edge [151–153].

The most frequent films used in solar cells are synthetic diamond films. A conventional diamond-based solar cell device might be made as follows: A diamond film is attached as the bottom layer on a metal sheet as the cathode, and then another sheet of electrically conducting material is put on top of the bottom diamond film, with a very small gap, between which all the air has been eliminated. It is simpler to use materials with a small bandgap in solar cells to absorb a wide spectrum of solar energy. The silicone layer absorbs the incident light while the rear side of the BDD layer is submerged in electrolytes as an anode with an electrically anti-corrosive long-term property [154]. Moreover, amorphous diamond films and diamond NP NDs demonstrate the benefit of turning heat or light into electric energy. This property allows for the use of amorphous diamond in thermal electric generators or solar cell arrays. However, despite the advantages of diamond-based solar cells, it was shown that, synthetic diamond generally has high electric resistance. Solar diamond-based cells will run too hot for manually running types of electronic devices, but there are no issues with large-scale energy converters for rooftops or solar-cell farms. Furthermore, highly doped diamonds

have less clarity to visible light, which limits their applications in solar cells [155].

For the construction of solar cells, heterojunctions use C_{60} and fullerenol (n-type), with the diamond and metal phthalocyanin derivatives (p-type). A benefit of using ND in solar cells is increase the amount of the p–n heterojunction interface. NDs were used as electron acceptor and porphyrin as electron donor to create solar systems. Photoactive reaction centres (RCs) is a novel scheme involving the use of high-performance biological units in bacteria or plants for solar energy conversion. The movement of electrons on nanocrystalline diamond anchored with functionalities of the bacterial RCs is greatly increased, thereby greatly increasing the production of photocurrent. Solar cells that use semi-conductive diamond and photo-reactive RCs functionalities as building units produce enhanced photocurrent, considered to be new types of bio solar cells. This bio solar cell's advantages will likely be realized by the use of synthetic diamond, which is used as a flexible medium for new functionalization [156].

Based on dye-sensitized colloidal TiO_2 films, a low-cost, high-efficiency solar cell has been developed by O'Regan and Grätzel [157]. The DSSC paved the way for more energy-efficient variants such as the perovskite solar cell [158] (PSC). Figure 8 illustrates that a coating of TiO_2 NPs is formed on which dye molecules are placed in a traditional DSC (a). When sunlight contacts the dye molecules, it produces both a negative charged electron (e) and a positive charged hole (h^+). The electron absorbed to an electrode through the TiO_2 coating and is then transported to a counter electrode. Finally, the electron enters a liquid electrolyte before recombining with the hole and being reabsorbed by the dye. The electrolyte is supplemented with a hole-transporting substance in a contemporary solid-state PSC (b), and chemical constituents called perovskites serve as light harvesters. To improve the effectiveness of PSCs, gold is typically utilized as the counter-electrode material.

8.2 Renewable energy

Nanotechnology has the ability to make inexpensive renewable energy resources greener have high efficient and high reliable. Among other renewable energy uses, NPs are used to increase wind and geothermal power generation and hydrogen fuel cells. Solar thermal energy storage can also be enhanced by using NPs. The topic of renewable energy is becoming increasingly relevant due to increased demand for electricity, volatility in the oil prices and environmental problems. New energy-generation technologies, such as solar and wind technologies,

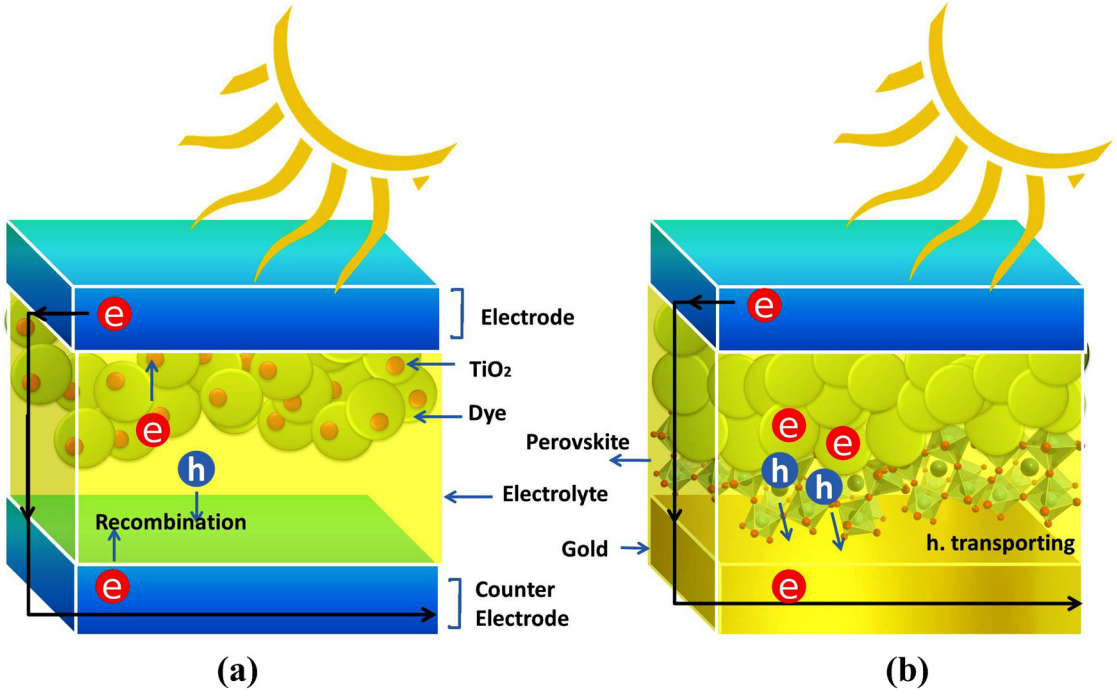

Figure 8: The difference between (a) the dye-sensitized solar cell (DSSC) and (b) the PSC.

have tremendous potential to reduce our reliance on energy generation systems that are on demand in real time. These current generation systems, however, are intermittent and sporadic; so, new types of effective, on-demand, energy storage systems are required to leverage green generation technologies to the maximum. Such technical demands drive the need for advanced electrochemical storage devices for electricity. There are two basic ways of storing or harnessing the energy that is contained in chemical bonds. The first is to sever the bonds, by means of a chemical or thermal process, and then capture the energy emitted in the form of heat and put it into practice [159]. By breaking those bonds and creating new bonds, a heat engine can absorb the energy that is stored in chemical bonds, and then use the excess energy that is produced from that process to do work. Therefore, as the heat energy taken from the source (the high-temperature tank) cannot be used to lower the temperature of the sink (the hypothermic tank) more than it already is, the amount of heat available to work will be limited by the energy difference between the source and the sink.

The absolute limit to engine output is determined by the temperature difference between the heat source and the heat sink. The ignition temperature in air for fuel is roughly 542 K. Assuming that the heat source is similar to that temperature, a heat engine's ideal maximum efficiency will be about 49%. Although this may seem fairly small, there is, however, a loss of energy in the form of heat being transmitted to the atmosphere (*i.e.* the walls) through convection, solid-state conduction, and the friction associated with piston movement. This energy loss decreases the kinetic energy of the gas particles generated from the combustion of the fuel, and the heat energy also increases the temperature of the sink/surroundings (the engine), thus the actual amount of work that can be achieved by gas expansion is further reduced. Conventional heat engines can also be used to produce electricity from chemical energy through an intermediate mechanical process. Because much of the energy emitted is not used in the form of heat, a system designed to capture the energy produced, such as a fuel cell, does not suffer the same restrictions as a Carnot heat engine on its operating capacity [159].

There are four major factors in real electrochemical devices, which decrease the device's open cell potential and operational potential. Such major factors are (1) mass concentration/transport losses, (2) activation losses, (3) ohmic losses, and (4) internal current losses. Activation losses arise from the need to resolve the energy activation barriers associated with the charging transfer reactions to ensure that the electrochemical reaction is channelled into product formation. At low current densities, those losses would have the most important effects. Such losses can be due to either the reverse electrochemical reaction, side redox reactions with either electrolyte materials, electrolyte pollutants, functional groups on the electrode surface, or unreacted fuel that can be attributable to physical losses, depending on the nature of the charge storage or generation processes associated with the system. The third type of loss is mass transport/concentration losses, which are most prevalent at high current densities. The final type and most common source of loss in any electrical device is ohmic losses. Such form of loss occurs due to the effect of the combined resistance inside the cell (separator, electrodes, and current collectors) and the interfaces between those components on the flow of electrons. All ohmic losses are directly proportional to the current. All these losses contribute in their own way to decrease the operational voltages in electrochemical devices. As we have already presented the Cu/Zn example cell that is indicative of a battery's operation, it may be best to continue with those cells. It operates much like a galvanic cell in the regular activity of a battery, in that electricity is produced as a result of a spontaneous chemical reaction.

The operating principles of fuel cells are similar to those batteries, in that redox processes are involved in electrical energy production. As the electricity production comes from a chemical reaction, fuel cells can be seen as acting similar to galvanic cells. At that viewpoint, with one important difference, fuel cells are like primary batteries: the electroactive species are not contained within a fuel cell but are supplied from external reservoirs. The hydrogen fuel cell is a prototype fuel cell that transforms hydrogen and oxygen straight into electricity, water, and some heat *via* reverse water hydrolysis. The hydrogen fuel is delivered to the anode, where it is oxidized, and the proton that results migrates to the cathode, where it is mixed with oxygen in a reduction process to generate liquid water.

Electrochemical capacitors are another method of storing energy in an electrochemical cell. It is energy storage by capability of double layers. Double layer capacitance in the form of electrostatic and electrolytic condensers has been known and exploited for several decades. These devices consist of two metal plates, which are separated by a dielectric. Electrical energy is generated by placing a charge on the electrodes (metal plates), which in turn creates a dielectric polarization between the plates. This accumulation of electrical charges contributes to the creation of an electrical field between the plates and has been traditionally referred to as dielectric storage. In parallel plate condensers, the thickness of the double layer forming between the dielectric polarized

molecules and the charged plate will be limited by the distance between the parallel charged plates. Therefore, the metal plate electrodes usually have a very small surface area, meaning that plate condensers or their modern counterparts generally have storage space [160].

8.3 Self-cleaning textiles

Both sustainable consumption and production are required improved consumption efficiency and a shift in consumption habits, as well as a reduction in consumption levels. Synthetic fibres, such as nylon and polyester that account for 60% of global clothing fibre, are frequently generated from non-renewable resources and harmful chemicals. More than 900 chemicals used in clothing production have been identified by the Swedish Chemicals Agency, of that 165 are listed by the EU as very harmful to human health or the environment [161]. The EU-27 textile consumption, of clothing is 70% by weight, produces a variety of effects throughout the life cycle. The phases of development and use control impacts, whereas their respective contributions to the different forms of impacts differ greatly. Reduced availability of water has an important impact on the nuclear and thermal power plants' hydropower and cooling [161].

In recent decades, the clothing and textile industry have globalized, driven largely by tariff liberalization and the related relocation of production to low labour-cost countries. Clothing has gotten cheaper in several European nations in the recent decade when compared to many other consumer items; in exporting countries, textile and clothing production often creates jobs [162]. In addition, to achieve environmental changes, the application of the recent developments in the manufacture of new textiles could be implemented. In the textile industry, nanotechnology has a high technological potential. Because NPs have a great area-to-volume ratio and a high surface energy, they can provide exceptional durability for textiles, resulting in a better affinity for textiles and resulting in an increase in functional durability. Furthermore, a NPs coating on textiles does not affect their scent or consumer contact. Therefore, the interest in the textile industry using nanotechnologies is increasing. The major application of this technology is a new concept for a washable and maintainable textile that may drastically improve process efficiency in terms of energy and resource use [163].

The new generation textile made through a finishing process would be capable of reducing the maintenance textile product costs, such as a significant reduction in water and chemical/detergent use, and substantially reducing the temperature needed to remove permanent stains. The new textile can be categorized as "self-cleaning textiles": they will produce a new industrial method for processing the textile itself and washing itself. In addition, the active compounds presence on the textile would cause the persistent stains to be decomposed by applying cycles of light washing and the number of surfactants, which will result in their easy removal. Washing machines that save energy are now available would have to be built and installed to optimize the benefits of the active compounds. By using nanotechnology, realizing self-cleaning qualities on textile surfaces opens up a world of possibilities for designers new materials or new applications for existing materials. Considering the possible toxicological hazards of releasing NPs in the atmosphere, there is no guarantee that the finished product can release a harmful amount of nano-TiO_2 to the atmosphere. The capacity of the revolutionary material to be washed lightly and less regularly was checked measuring a reduction in the use of tap water. This specific environmental dimension also depends on the washing cycles number. Results demonstrate that creative textile finishing provides significant benefits in terms of water consumption reduction [161,162].

Preparing TiO_2 NPs is the focus of recent attempts to improve photocatalytic activity of TiO_2 NPs and generate self-cleaning textiles have antibacterial and antifungal. Ghobashy *et al.* prepared fabric of polyethylene terephthalate (PET) composite with TiO_2 NPs using gamma irradiation techniques as green synthesis route. The obtained data showed that the new fabric nanocomposite of PET@TiO_2 has a self-cleaning character, which depends on the water vapour in air and light of sun [99].

The attachment of TiO_2 NPs to two-dimensional graphene nanosheets has been characterized in several techniques. For instance, free electrons on the TiO_2 surface can be bonded to produce a TieOeC nanocomposite containing unpaired carbon atoms. Owing to the tightly conjugated graphene structure producing TieOeC chemical bonds and the removal of TiO_2 band gaps due to carbon doping, these composites optimize wavelength absorption spectrum in visible region [164].

Stan *et al.* [165] manufactured cotton fibres treated with rGO decorated with Fe-doped, N-doped TiO_2 NPs. Several strategies have been developed to make photocatalytic self-cleaning textiles and have antimicrobial activity under visible light, the textile was made from TiO_2 nanoparticles alone or doped with different nonmetals [166,167]. The improved properties of rGO-treated fibres of cotton decorated with doped of Fe-, N- with TiO_2 NPs to be used as industrial self-cleaning textiles.

Cashew nut liquid shells are proposed as a possible sustainable and green raw material for synthetic dyes [168]. Perchloroethylene (PERC) is a compound widely used in dry cleaning as a solvent, given its significant safety and environmental impacts. PERC compound was used as a solvent in professional dry cleaners. PERC has serious implications for health and the environment. In recent years, less damaging alternatives to PERC have evolved, such as hydrocarbons, green clay, vinyl acetate, and liquid CO_2, and a potential water-based wet cleaning technique has been established. Wet textile washing is gaining traction as a viable alternative to dry cleaning regarding the environmental acceptability, lack of hazardous chemicals, and satisfactory cleaning results [169].

9 Advantages of the gamma irradiation techniques

As gamma irradiation technique of the radiolytic synthesis is used to develop new and optimized ways of NP synthesis, they have several advantages that may be seen when compared to other approaches or traditional green technologies, such as higher quantities of monosized and highly monodispersed metal clusters with very low of energy required. The radiolytic synthesis is carried out at ambient temperature and ambient pressure settings, without the need of chemical reducing agents, and with high stability and reliability. The control of different experimental parameters (such as irradiation doses, solvent, pH and procurers concentrations) allows for the NP manufacture with high purity, as well as the control of NP size and their structure. If the irradiation procedure is properly done and regulated, no residuals or related product damage should be expected. Furthermore, the ability to combine sterilization process and NP production in a single operation is a unique benefit that gamma irradiation synthesis may provide. This benefit is even more significant if the created system matches to the final product to be sold because radiation may be done inside the final package, preventing further pollution and handling.

10 Conclusion

The concept of green chemistry is environmentally friendly processes and technologies improved and used so that the environment is not unregulated, and natural resources are preserved. Often this technology means software that uses innovative methods to produce environmentally friendly goods. This primarily includes many everyday cleaning items, waste, technology, energy sources, clothing, and a host of others. Going green or using environmentally friendly technology is one of the many strategies that countries are trying to promote economic development and improve the lives of their citizens. An environmentally sustainable life is an optimistic goal. Green biosynthesis has been extensively explored by numerous researcher nowadays, and it was chosen as an alternative route to produce a safe and eco-friendly NPs. Preparation using green substrates such as plant-based extract, microorganism, biopolymer, and carbohydrate are much more preferable nowadays in order to save the environment by reducing the involvement of toxic chemicals. The production of NPs from natural extracts is gaining more focus in nanotechnology. The biosynthesis process for green NPs production occurs by simultaneous effect of microorganisms extract or plant extract on ions solution, which simultaneously forms NP at high temperature and high pressure or microwave assist. The resulting NP are formed much quicker when compared to other NP synthesis. For biological and medicinal applications where NP purity is critical, the utilization of natural resources for NP synthesis is sustainable, eco-friendly, cheap, and devoid of chemical contamination. On a big scale, useful and common nanomaterials may be easily manufactured. Biological techniques do not necessitate the use of harsh or harmful chemicals. Plant extracts are not easy to get rid of. Furthermore, as compared to physicochemical techniques, NPs generated using the green way are more stable and effective. Many efforts have been made to produce secondary metabolites from natural product extracts that might be used as reducing, stabilizing, and capping agents in the nanomaterials production process. Capping and stabilizing compounds found in biological entities function as growth inhibitors, inhibiting agglomeration processes and improving NP stability and persistence. The size and form of NPs are influenced by the nature of biological entities at varying concentrations with a mix of organic reducing agents. This review represent the using of gamma irradiation-based green approach to prepare a high yield of NPs with a narrow size distribution offers significant benefits, as evidenced by UV/Vis spectra and TEM pictures. Show also the effect of irradiation doses, solvent, and pH of reaction media on the shape and size of obtained NPs.

Funding information: The authors state no funding involved.

Author contributions: All authors have accepted responsibility for the entire content of this manuscript and approved its submission.

Conflict of interest: The authors state no conflict of interest.

References

[1] Anastas P, Williamson T. Green chemistry-designing chemistry for the environment. ACS Symoposium Series 626th. Washington, DC: American Chemical Society; 1996.

[2] Anastas P, Eghbali N. Green chemistry: principles and practice. Chem Soc Rev. 2010;39(1):301–12.

[3] Raveendran P, Fu J, Wallen SL. Completely "green" synthesis and stabilization of metal nanoparticles. J Am Chem Soc. 2003;125(46):13940–1.

[4] Gils PS, Ray D, Sahoo PK. Designing of silver nanoparticles in gum arabic based semi-IPN hydrogel. Int J Biol macromolecules. 2010;46(2):237–44.

[5] Modrzejewska Z, Zarzycki R, Sielski J. Synthesis of silver nanoparticles in a chitosan solution. Prog Chem Appl Chitin Derivatives. 2010;15:63–72.

[6] Kora AJ, Sashidhar RB, Arunachalam J. Gum Kondagogu (*Cochlospermum gossypium*): a template for the green synthesis and stabilization of silver nanoparticles with antibacterial application. Carbohydr Polym. 2010;82(3):670–9.

[7] Mohan YM, Raju KM, Sambasivudu K, Singh S, Sreedhar B. Preparation of acacia-stabilized silver nanoparticles: a green approach. J Appl Polym Sci. 2007;106(5):3375–81.

[8] Kemp MM, Kumar A, Mousa S, Dyskin E, Yalcin M, Ajayan P, et al. Gold and silver nanoparticles conjugated with heparin derivative possess anti-angiogenesis properties. Nanotechnology. 2009;20(45):455104.

[9] Pandey S, Goswami GK, Nanda KK. Green synthesis of biopolymer–silver nanoparticle nanocomposite: an optical sensor for ammonia detection. Int J Biol Macromol. 2012;51(4):583–9.

[10] Horváth IT, Anastas PT. Introduction: green chemistry. New Haven, CT, USA: ACS Publications; 2007.

[11] Anastas PT, Warner JC. Green chemistry: theory and practice. New York: Oxford University Press; 1998.

[12] Zhang Y. Discussion on the development of green chemistry and chemical engineering. IOP Conference Series: Earth and Environmental Science; 2017. p. 012136.

[13] Stubbs D, Gilman P. Nanotechnology applications in environmental health: big plans for little particles. Oak Ridge: Oak Ridge Center for Advanced Studies; 2007.

[14] Restrepo CV, Villa CC. Synthesis of silver nanoparticles, influence of capping agents, and dependence on size and shape: a review. Environ Nanotechnol Monit Manag. 2021;15:100428.

[15] Garg A, Rai G, Lodhi S, Jain AP, Yadav AK. *In-vitro* and *in-vivo* assessment of dextran-appended cellulose acetate phthalate nanoparticles for transdermal delivery of 5-fluorouracil. Drug Delivery. 2016;23(5):1525–35.

[16] Gericke M, Schulze P, Heinze T. Nanoparticles based on hydrophobic polysaccharide derivatives – formation principles, characterization techniques, and biomedical applications. Macromol Biosci. 2020;20(4):1900415.

[17] Banerjee A, Das D, Andler R, Bandopadhyay R. Green synthesis of silver nanoparticles using exopolysaccharides produced by Bacillus anthracis PFAB2 and its biocidal property. J Polym Environ. 2021;29:1–9.

[18] İspirli H, Sagdic O, Dertli E. Synthesis of silver nanoparticles prepared with a dextran-type exopolysaccharide from Weissella cibaria MED17 with antimicrobial functions. Prep Biochem Biotechnol. 2021;51(2):112–9.

[19] Ashtiyani MK, Hajipour-Verdom B, Satari M, Abdolmaleki P, Hosseinkhani S. Estimating the two graph dextran-stearic acid-spermine polymers based on iron oxide nanoparticles as carrier for gene delivery. 2021.

[20] Zhao C-L, Gao Y-Z, Wu M-Y, Zhang H-T, Wu Y-X. Biocompatible, hemocompatible and antibacterial acylated dextran-*g*-polyisobutylene graft copolymers with silver nanoparticles. Chin J Polym Sci. 2021;39:1550–61.

[21] Anghelache M, Turtoi M, Petrovici AR, Fifere A, Pinteala M, Calin M. Development of dextran-coated magnetic nanoparticles loaded with protocatechuic acid for vascular inflammation therapy. Pharmaceutics. 2021;13(9):1414.

[22] Yu M, Huang S, Yu KJ, Clyne AM. Dextran and polymer polyethylene glycol (PEG) coating reduce both 5 and 30 nm iron oxide nanoparticle cytotoxicity in 2D and 3D cell culture. Int J Mol Sci. 2012;13(5):5554–70.

[23] Esfahani AR, Sadiq Z, Oyewunmi OD, Tali SHS, Usen N, Boffito DC, et al. Portable, stable, and sensitive assay to detect phosphate in water with gold nanoparticles (AuNPs) and dextran tablet. Analyst. 2021;146(11):3697–708.

[24] Kokilavani S, Syed A, Thomas AM, Elgorban AM, Bahkali AH, Marraiki N, et al. Development of multifunctional Cu sensitized Ag-dextran nanocomposite for selective and sensitive detection of mercury from environmental sample and evaluation of its photocatalytic and anti-microbial applications. J Mol Liq. 2021;321:114742.

[25] Bevacqua E, Curcio M, Saletta F, Vittorio O, Cirillo G, Tucci P. Dextran-curcumin nanosystems inhibit cell growth and migration regulating the epithelial to mesenchymal transition in prostate cancer cells. Int J Mol Sci. 2021;22(13):7013.

[26] El Founi M, Laroui H, Canup BSB, Ametepe JS, Vanderesse R, Acherar S, et al. Doxorubicin intracellular release *via* external UV irradiation of dextran-*g*-poly (*o*-nitrobenzyl acrylate) photosensitive nanoparticles. ACS Appl Bio Mater. 2021;4(3):2742–51.

[27] Das M, Oyarzabal EA, Chen L, Lee S-H, Shah N, Gerlach G, et al. One-pot synthesis of carboxymethyl-dextran coated iron oxide nanoparticles (CION) for preclinical fMRI and MRA applications. NeuroImage. 2021;238:118213.

[28] Popov A, Abakumov MA, Savintseva I, Ermakov A, Popova N, Ivanova O, et al. Biocompatible dextran-coated gadolinium-doped cerium oxide nanoparticles as MRI contrast agents with high T1 relaxivity and selective cytotoxicity to cancer cells. J Mater Chem B. 2021;9:6586–99.

[29] Amin RM, Taha M, Moaty SAA, El-Ela FIA, Nassar HF, GadelHak Y, et al. Gamma radiation as a green method to enhance the dielectric behaviour, magnetization,

antibacterial activity and dye removal capacity of Co–Fe LDH nanosheets. RSC Adv. 2019;9(56):32544–61.
[30] Tang J, Fu X, Ou Q, Gao K, Man S-Q, Guo J, et al. Hydroxide assisted synthesis of monodisperse and biocompatible gold nanoparticles with dextran. Mater Sci Eng: C. 2018;93:759–67.
[31] Hien NQ, Tuan PD, Van Phu D, Lan NTK, Duy NN, Hoa TT. Gamma Co-60 ray irradiation synthesis of dextran stabilized selenium nanoparticles and their antioxidant activity. Mater Chem Phys. 2018;205:29–34.
[32] Phan TTV, Hoang G, Nguyen TP, Kim HH, Mondal S, Manivasagan P, et al. Chitosan as a stabilizer and size-control agent for synthesis of porous flower-shaped palladium nanoparticles and their applications on photo-based therapies. Carbohydr Polym. 2019;205:340–52.
[33] Kalaivani R, Maruthupandy M, Muneeswaran T, Beevi AH, Anand M, Ramakritinan CM, et al. Synthesis of chitosan mediated silver nanoparticles (Ag NPs) for potential antimicrobial applications. Front Lab Med. 2018;2(1):30–5.
[34] Phan TTV, Ahn S-H, Oh J. Chitosan-mediated facile green synthesis of size-controllable gold nanostars for effective photothermal therapy and photoacoustic imaging. Eur Polym J. 2019;118:492–501.
[35] Phan TTV, Phan DT, Cao XT, Huynh T-C, Oh J. Roles of chitosan in green synthesis of metal nanoparticles for biomedical applications. Nanomaterials. 2021;11(2):273.
[36] Grzelczak M, Pérez-Juste J, Mulvaney P, Liz-Marzán LM. Shape control in gold nanoparticle synthesis. Chem Soc Rev. 2008;37(9):1783–91.
[37] Zhao L, Jiang D, Cai Y, Ji X, Xie R, Yang W. Tuning the size of gold nanoparticles in the citrate reduction by chloride ions. Nanoscale. 2012;4(16):5071–6.
[38] Ding Y, Gu G, Xia X-H, Huo Q. Cysteine-grafted chitosan-mediated gold nanoparticle assembly: from nanochains to microcubes. J Mater Chem. 2009;19(6):795–9.
[39] Luesakul U, Komenek S, Puthong S, Muangsin N. Shape-controlled synthesis of cubic-like selenium nanoparticles *via* the self-assembly method. Carbohydr Polym. 2016;153:435–44.
[40] Creixell M, Herrera AP, Latorre-Esteves M, Ayala V, Torres-Lugo M, Rinaldi C. The effect of grafting method on the colloidal stability and *in vitro* cytotoxicity of carboxymethyl dextran coated magnetic nanoparticles. J Mater Chem. 2010;20(39):8539–47.
[41] Maslamani N, Khan SB, Danish EY, Bakhsh EM, Zakeeruddin SM, Asiri AM. Carboxymethyl cellulose nanocomposite beads as super-efficient catalyst for the reduction of organic and inorganic pollutants. Int J Biol Macromol. 2021;167:101–16.
[42] Salehi AA, Ghannadi-Maragheh M, Torab-Mostaedi M, Torkaman R, Asadollahzadeh M. Hydrogel materials as an emerging platform for desalination and the production of purified water. Sep Purif Rev. 2021;50(4):380–99.
[43] Nadagouda MN, Varma RS. Synthesis of thermally stable carboxymethyl cellulose/metal biodegradable nanocomposites for potential biological applications. Biomacromolecules. 2007;8(9):2762–7.
[44] He F, Zhao D, Liu J, Roberts CB. Stabilization of Fe–Pd nanoparticles with sodium carboxymethyl cellulose for enhanced transport and dechlorination of trichloroethylene in soil and groundwater. Ind Eng Chem Res. 2007;46(1):29–34.
[45] He F, Liu J, Roberts CB, Zhao D. One-step "green" synthesis of Pd nanoparticles of controlled size and their catalytic activity for trichloroethene hydrodechlorination. Ind Eng Chem Res. 2009;48(14):6550–7.
[46] Liu J, Sutton J, Roberts CB. Synthesis and extraction of monodisperse sodium carboxymethylcellulose-stabilized platinum nanoparticles for the self-assembly of ordered arrays. J Phys Chem C. 2007;111(31):11566–76.
[47] Asghar MA, Yousuf RI, Shoaib MH, Asghar MA, Zehravi M, Rehman AA, et al. Green synthesis and characterization of carboxymethyl cellulose fabricated silver-based nanocomposite for various therapeutic applications. Int J Nanomed. 2021;16:5371.
[48] Khan A, Alamry KA, Oves M, Althomali RH. A facile and green approach for the fabrication of nano-biocomposites by reducing silver salt solution into silver nanoparticles using modified carboxymethyl cellulose for antimicrobial potential. J Polym Res. 2021;28(3):1–13.
[49] Raghu Babu K, Kumar J, Suseela Bai G, Singh J, Reddy V. Carboxymethyl cellulose stabilized lead sulfide nanocrystals: synthesis, characterization and catalytic applications. Colloids Surf A: Physicochem Eng Asp. 2021;620:126572.
[50] Silva Viana RL, Pereira Fidelis G, Jane Campos Medeiros M, Antonio Morgano M, Gabriela Chagas Faustino Alves M, Domingues Passero LF, et al. Green synthesis of antileishmanial and antifungal silver nanoparticles using corn cob xylan as a reducing and stabilizing agent. Biomolecules. 2020;10(9):1235.
[51] Brito TK, Viana RLS, Moreno CJG, da Silva Barbosa J, de Sousa Júnior FL, de Medeiros MJC, et al. Synthesis of silver nanoparticle employing corn cob xylan as a reducing agent with anti-Trypanosoma cruzi activity. Int J Nanomed. 2020;15:965.
[52] Feng X, Guangda H, Jihai C, Xiaoying W. Au@ Carbon quantum Dots-MXene nanocomposite as an electrochemical sensor for sensitive detection of nitrite. J Colloid Interface Sci. 2022;607:1313–22.
[53] Cai J, Han G, Ren J, Liu C, Wang J, Wang X. Single-layered graphene quantum dots with self-passivated layer from xylan for visual detection of trace chromium(VI). Chem Eng J. 2021;436:131833.
[54] Han G, Cai J, Liu C, Ren J, Wang X, Yang J, et al. Highly sensitive electrochemical sensor based on xylan-based Ag@ CQDs-rGO nanocomposite for dopamine detection. Appl Surf Sci. 2021;541:148566.
[55] Cai J, Li Y, Liu C, Wang X. Green and controllable synthesis of Au–Ag bimetal nanoparticles by xylan for surface-enhanced Raman scattering. ACS Sustain Chem Eng. 2019;7(18):15154–62.
[56] Immerzeel P, Falck P, Galbe M, Adlercreutz P, Karlsson EN, Stålbrand H. Extraction of water-soluble xylan from wheat bran and utilization of enzymatically produced xylooligosaccharides by Lactobacillus, Bifidobacterium and Weissella spp. LWT-Food Sci Technol. 2014;56(2):321–7.
[57] Harish BS, Uppuluri KB, Anbazhagan V. Synthesis of fibrinolytic active silver nanoparticle using wheat bran xylan as a reducing and stabilizing agent. Carbohydr Polym. 2015;132:104–10.

[58] Luo Y, Shen S, Luo J, Wang X, Sun R. Green synthesis of silver nanoparticles in xylan solution *via* Tollens reaction and their detection for Hg^{2+}. Nanoscale. 2015;7(2):690–700.
[59] Pourreza N, Golmohammadi H, Naghdi T, Yousefi H. Green *in-situ* synthesized silver nanoparticles embedded in bacterial cellulose nanopaper as a bionanocomposite plasmonic sensor. Biosens Bioelectron. 2015;74:353–9.
[60] Pérez-Alvarez M, Cadenas-Pliego G, Pérez-Camacho O, Comparán-Padilla VE, Cabello-Alvarado CJ, Saucedo-Salazar E. Green synthesis of copper nanoparticles using cotton. Polymers. 2021;13(12):1906.
[61] Heidari H, Karbalaee M. Ultrasonic assisted synthesis of nanocrystalline cellulose as support and reducing agent for Ag nanoparticles: green synthesis and novel effective nanocatalyst for degradation of organic dyes. Appl Organomet Chem. 2019;33(9):e5070.
[62] Lokanathan AR, Nykänen A, Seitsonen J, Johansson L-S, Campbell J, Rojas OJ, et al. Cilia-Mimetic hairy surfaces based on end-immobilized nanocellulose colloidal rods. Biomacromolecules. 2013;14(8):2807–13.
[63] Bohrn R, Potthast A, Schiehser S, Rosenau T, Sixta H, Kosma P. The FDAM method: determination of carboxyl profiles in cellulosic materials by combining group-selective fluorescence labeling with GPC. Biomacromolecules. 2006;7(6):1743–50.
[64] Quesenberry MS, Lee YC. A simple spectrophotometric method for estimation of peroxidase activity in blood samples. Anal Biochem. 1996;234:50–5.
[65] Röhrling J, Potthast A, Rosenau T, Lange T, Ebner G, Sixta H, et al. A novel method for the determination of carbonyl groups in cellulosics by fluorescence labeling. 1. Method Dev Biomacromol. 2002;3(5):959–68.
[66] Tang C, Spinney S, Shi Z, Tang J, Peng B, Luo J, et al. Amphiphilic cellulose nanocrystals for enhanced pickering emulsion stabilization. Langmuir. 2018;34(43):12897–905.
[67] Ahlgren PA, Goring DAI. Removal of wood components during chlorite delignification of black spruce. Can J Chem. 1971;49(8):1272–5.
[68] Pollet P, Eckert CA, Liotta CL. Solvents for sustainable chemical processes. WIT Trans Ecol Env. 2011;154:21–31.
[69] Fürstner A, Ackermann L, Beck K, Hori H, Koch D, Langemann K, et al. Olefin metathesis in supercritical carbon dioxide. J Am Chem Soc. 2001;123(37):9000–6.
[70] Wittmann K, Wisniewski W, Mynott R, Leitner W, Kranemann CL, Rische T, et al. Supercritical carbon dioxide as solvent and temporary protecting group for rhodium-catalyzed hydroaminomethylation. Chem–A Eur J. 2001;7(21):4584–9.
[71] Ohde H, Hunt F, Wai CM. Synthesis of silver and copper nanoparticles in a water-in-supercritical-carbon dioxide microemulsion. Chem Mater. 2001;13(11):4130–5.
[72] Sue K, Adschiri T, Arai K. Predictive model for equilibrium constants of aqueous inorganic species at subcritical and supercritical conditions. Ind & Eng Chem Res. 2002;41(13):3298–306.
[73] Kim M, Lee BY, Ham HC, Han J, Nam SW, Lee H-S, et al. Facile one-pot synthesis of tungsten oxide (WO_{3-x}) nanoparticles using sub and supercritical fluids. J Supercrit Fluids. 2016;111:8–13.
[74] Xu C, Lee J, Teja AS. Continuous hydrothermal synthesis of lithium iron phosphate particles in subcritical and supercritical water. J Supercrit Fluids. 2008;44(1):92–7.
[75] DeSimone JM. Practical approaches to green solvents. Science. 2002;297(5582):799–803.
[76] Er H, Yasuda H, Harada M, Taguchi E, Iida M. Formation of silver nanoparticles from ionic liquids comprising *N*-alkylethylenediamine: effects of dissolution modes of the silver (I) ions in the ionic liquids. Colloids Surf A: Physicochem Eng Asp. 2017;522:503–13.
[77] Srivastava V. *In situ* generation of Ru nanoparticles to catalyze CO_2 hydrogenation to formic acid. Catal Lett. 2014;144(10):1745–50.
[78] Vollmer C, Redel E, Abu-Shandi K, Thomann R, Manyar H, Hardacre C, et al. Microwave irradiation for the facile synthesis of transition-metal nanoparticles (NPs) in ionic liquids (ILs) from metal–carbonyl precursors and Ru-, Rh-, and Ir-NP/IL dispersions as biphasic liquid–liquid hydrogenation nanocatalysts for cyclohexene. Chem–A Eur J. 2010;16(12):3849–58.
[79] Zhang H, Cui H. Synthesis and characterization of functionalized ionic liquid-stabilized metal (gold and platinum) nanoparticles and metal nanoparticle/carbon nanotube hybrids. Langmuir. 2009;25(5):2604–12.
[80] Zhang ZC. Catalysis in ionic liquids. Adv Catal. 2006;49:153–237.
[81] Dupont J, de Souza RF, Suarez PAZ. Ionic liquid (molten salt) phase organometallic catalysis. Chem Rev. 2002;102(10):3667–92.
[82] Van Rantwijk F, Sheldon RA. Biocatalysis in ionic liquids. Chem Rev. 2007;107(6):2757–85.
[83] Welton T. Ionic liquids in catalysis. Coord Chem Rev. 2004;248(21–24):2459–77.
[84] Bussamara R, Melo WWM, Scholten JD, Migowski P, Marin G, Zapata MJM, et al. Controlled synthesis of Mn_3O_4 nanoparticles in ionic liquids. Dalton Trans. 2013;42(40):14473–9.
[85] Lazarus LL, Riche CT, Malmstadt N, Brutchey RL. Effect of ionic liquid impurities on the synthesis of silver nanoparticles. Langmuir. 2012;28(45):15987–93.
[86] Li N, Bai X, Zhang S, Ya G, Zheng, Zhang L, J, et al. Synthesis of silver nanoparticles in ionic liquid by a simple effective electrochemical method. J Dispers Sci Technol. 2008;29(8):1059–61.
[87] Kim K-S, Demberelnyamba D, Lee H. Size-selective synthesis of gold and platinum nanoparticles using novel thiol-functionalized ionic liquids. Langmuir. 2004;20(3):556–60.
[88] Dupont J, Fonseca GS, Umpierre AP, Fichtner PFP, Teixeira SR. Transition-metal nanoparticles in imidazolium ionic liquids: recycable catalysts for biphasic hydrogenation reactions. J Am Chem Soc. 2002;124(16):4228–9.
[89] Bouquillon S, Courant T, Dean D, Gathergood N, Morrissey S, Pegot B, et al. Biodegradable ionic liquids: selected synthetic applications. Aust J Chem. 2007;60(11):843–7.
[90] Carter EB, Culver SL, Fox PA, Goode RD, Ntai I, Tickell MD, et al. Sweet success: ionic liquids derived from non-nutritive sweeteners. Chem Commun. 2004;6:630–1.
[91] Harjani JR, Singer RD, Garcia MT, Scammells PJ. Biodegradable pyridinium ionic liquids: design, synthesis and evaluation. Green Chem. 2009;11(1):83–90.

[92] Imperato G, Koenig B, Chiappe C. Ionic green solvents from renewable resources. Eur J Org Chem. 2007;2007(7):1049–58.
[93] Ghobashy MM, El-Sattar NEAA. Radiation synthesis of rapidly self-healing hydrogel derived from poly (acrylic acid) with good mechanical strength. Macromol Chem Phys. 2020;221(19):2000218.
[94] Ghobashy MM, Alshangiti DM, Alkhursani SA, Al-Gahtany SA, Shokr FS, Madani M. Improvement of *in vitro* dissolution of the poor water-soluble amlodipine drug by solid dispersion with irradiated polyvinylpyrrolidone. ACS Omega. 2020;5(34):21476–87.
[95] Elhady MA, Ghobashy MM, Mahmoud MA. Effect of gamma irradiation on the adhesive property and antibacterial activity of blend polymer (abietic acid-EVA). Polym Compos. 2020;29:138–47.
[96] Alshangiti DM, Ghobashy MM, Alkhursani SA, Shokr FS, Al-Gahtany SA, Madani MM. Semi-permeable membrane fabricated from organoclay/PS/EVA irradiated by ɣ-rays for water purification from dyes. J Mater Res Technol. 2019;8(6):6134–45.
[97] Ghobashy MM, Alkhursani SA, Madani M. Radiation-induced nucleation and pH-controlled nanostructure shape of polyaniline dispersed in DMF. Polym Bull. 2018;75(12):5477–92.
[98] Ghobashy MM, Elhady MA. pH-sensitive wax emulsion copolymerization with acrylamide hydrogel using gamma irradiation for dye removal. Radiat Phys Chem. 2017;134:47–55.
[99] Ghobashy MM. Combined ultrasonic and gamma-irradiation to prepare TiO_2@ PET-*g*-PAAc fabric composite for self-cleaning application. Ultrason Sonochem. 2017;37:529–35.
[100] Ghobashy MM, El-Damhougy BK, El-Wahab HA, Madani M, Amin MA, Naser AEM, et al. Controlling radiation degradation of a CMC solution to optimize the swelling of acrylic acid hydrogel as water and fertilizer carriers. Polym Adv Technol. 2021;32(2):514–24.
[101] Ghobashy MM, El-Sawy NM, Kodous AS. Nanocomposite of cosubstituted carbonated hydroxyapatite fabricated inside poly (sodium hyaluronate-acrylamide) hydrogel template prepared by gamma radiation for osteoblast cell regeneration. Radiat Phys Chem. 2021;109408.
[102] Ghobashy MM, Khafaga MR. Chemical modification of nano polyacrylonitrile prepared by emulsion polymerization induced by gamma radiation and their use for removal of some metal ions. J Polym Environ. 2017;25(2):343–8.
[103] Le Caër S. Water radiolysis: influence of oxide surfaces on H2 production under ionizing radiation. Water. 2011;3(1):235–53.
[104] Bockris JM, Oldfield LF. The oxidation-reduction reactions of hydrogen peroxide at inert metal electrodes and mercury cathodes. Trans Faraday Soc. 1955;51:249–59.
[105] Strbac S. The effect of pH on oxygen and hydrogen peroxide reduction on polycrystalline Pt electrode. Electrochim Acta. 2011;56(3):1597–604.
[106] Torres CRG, Crastechini E, Feitosa FA, Pucci CR, Borges AB. Influence of pH on the effectiveness of hydrogen peroxide whitening. Operative Dent. 2014;39(6):E261–E8.
[107] Hori T, Nagata K, Iwase A, Hori F. Synthesis of Cu nanoparticles using gamma-ray irradiation reduction method. Jpn J Appl Phys. 2014;53(5S1):05FC.
[108] Dey GR. Reduction of the copper ion to its metal and clusters in alcoholic media: a radiation chemical study. Radiat Phys Chem. 2005;74(3–4):172–84.
[109] Ershov BG. Radiation-induced oxidation of iron in the ocean of the early Earth. Precambrian Res. 2021;364:106360.
[110] Alrehaily LM. Gamma-radiation induced redox reactions and colloidal formation of chromium and cobalt oxide nanoparticles. NY, USA: Elsevier; 2015.
[111] O'Connor CJ, Hormes J, Bazan NG. Bio-magnetics interfacing concepts: a microfluidic system using magnetic nanoparticles for quantitative detection of biological species. NEW Orleans University La Advanced Materials Research Institute; 2004.
[112] Gracien EB, Jérémie ML, Joseph LK-K, Omer MM, Antoine MK, Hercule KM, et al. Role of hydroxyl radical scavenger agents in preparing silver nanoparticles under γ-irradiation. SN Appl Sci. 2019;1(9):1–8.
[113] Isherwood LH, Athwal G, Spencer BF, Casiraghi C, Baidak A. Gamma radiation-induced oxidation, doping, and etching of two-dimensional MOS_2 crystals. J Phys Chem C. 2021;125(7):4211–22.
[114] Mohamady Ghobashy M, Sayed WAA, El-Helaly A. Impact of silver nanoparticles synthesized by irradiated polyvinylpyrrolidone on spodoptera littoralis nucleopolyhedrosis virus activity. J Polym Environ. 2021;29:3364–74.
[115] Korolkov IV, Güven O, Mashentseva AA, Atıcı AB, Gorin YG, Zdorovets MV, et al. Radiation induced deposition of copper nanoparticles inside the nanochannels of poly (acrylic acid)-grafted poly (ethylene terephthalate) track-etched membranes. Radiat Phys Chem. 2017;130:480–7.
[116] Kraynov A, Müller TE. Applications of ionic liquids in science and technology. Rijeka, Croatia: InTech Open; 2011.
[117] Belloni J. Nucleation, growth and properties of nanoclusters studied by radiation chemistry: application to catalysis. Catal Today. 2006;113(3–4):141–56.
[118] Phu DV, Lang VTK, Kim Lan NT, Duy NN, Chau ND, Du BD, et al. Synthesis and antimicrobial effects of colloidal silver nanoparticles in chitosan by γ-irradiation. J Exp Nanosci. 2010;5(2):169–79.
[119] Li T, Park HG, Choi S-H. γ-Irradiation-induced preparation of Ag and Au nanoparticles and their characterizations. Mater Chem Phys. 2007;105(2–3):325–30.
[120] Vo KDN, Kowandy C, Dupont L, Coqueret X, Hien NQ. Radiation synthesis of chitosan stabilized gold nanoparticles comparison between e^- beam and γ irradiation. Radiat Phys Chem. 2014;94:84–7. doi: 10.1016/j.radphyschem.2013.04.015.
[121] Mostafavi M, Marignier JL, Amblard J, Belloni J. Nucleation dynamics of silver aggregates simulation of photographic development processes. Int J Radiat Appl Instrum Part C Radiat Phys Chem. 1989;34(4):605–17.
[122] Belloni J. Metal nanocolloids. Curr Opcolloid Interface Sci. 1996;1(2):184–96.
[123] Balcerzyk A, Schmidhammer U, Horne G, Wang F, Ma J, Pimblott SM, et al. Unexpected ultrafast silver ion reduction: dynamics driven by the solvent structure. J Phys Chem B. 2015;119(31):10096–101.
[124] Dey GR, El Omar AK, Jacob JA, Mostafavi M, Belloni J. Mechanism of trivalent gold reduction and reactivity of transient divalent and monovalent gold ions studied by

gamma and pulse radiolysis. J Phys Chem A. 2011;115(4):383–91.
[125] Sapurina I, Stejskal J. The mechanism of the oxidative polymerization of aniline and the formation of supramolecular polyaniline structures. Polym Int. 2008;57(12):1295–325.
[126] Liu Q-M, Yasunami T, Kuruda K, Okido M. Preparation of Cu nanoparticles with ascorbic acid by aqueous solution reduction method. Trans Nonferrous Met Soc China. 2012;22(9):2198–203.
[127] Ramnani SP, Biswal J, Sabharwal S. Synthesis of silver nanoparticles supported on silica aerogel using gamma radiolysis. Radiat Phys Chem. 2007;76(8–9):1290–4.
[128] Wu M-L, Chen D-H, Huang T-C. Synthesis of Au/Pd bimetallic nanoparticles in reverse micelles. Langmuir. 2001;17(13):3877–83.
[129] Rao YN, Banerjee D, Datta A, Das SK, Guin R, Saha A. Gamma irradiation route to synthesis of highly re-dispersible natural polymer capped silver nanoparticles. Radiat Phys Chem. 2010;79(12):1240–6.
[130] Abedini A, Menon PS, Daud AR, Hamid MAA, Shaari S. Radiolytic formation of highly luminescent triangular Ag nanocolloids. J Radioanal Nucl Chem. 2016;307(2):985–91.
[131] Ansari SH, Islam F, Sameem M. Influence of nanotechnology on herbal drugs: a review. J Adv Pharm Technol Res. 2012;3(3):142.
[132] Hajialyani M, Tewari D, Sobarzo-Sánchez E, Nabavi SM, Farzaei MH, Abdollahi M. Natural product-based nanomedicines for wound healing purposes: therapeutic targets and drug delivery systems. Int J Nanomed. 2018;13:5023.
[133] Zhang J, Hu K, Di L, Wang P, Liu Z, Zhang J, et al. Traditional herbal medicine and nanomedicine: converging disciplines to improve therapeutic efficacy and human health. Adv Drug Delivery Rev. 2021;178:113964.
[134] Zhang Y. Discussion on the development of green chemistry and chemical engineering. 1st edn. Singapore: IOP Publishing; p. 012136.
[135] Bashir AKH, Matinise N, Sackey J, Kaviyarasu K, Madiba IG, Kodseti L, et al. Investigation of electrochemical performance, optical and magnetic properties of NiFe2O4 nanoparticles prepared by a green chemistry method. Phys E: Low-Dimens Syst Nanostruct. 2020;119:114002.
[136] Ramanarayanan R, Chokiveetil N, Pullanjiyot N, Meethal BN, Swaminathan S. The deterministic role of resonance energy transfer in the performance of bio-inspired colloidal silver nanoparticles incorporated dye sensitized solar cells. Mater Res Bull. 2019;114:28–36.
[137] Ng K, Webster M, Carbery WP, Visaveliya N, Gaikwad P, Jang SJ, et al. Frenkel excitons in heat-stressed supramolecular nanocomposites enabled by tunable cage-like scaffolding. Nat Chem. 2020;12(12):1157–64.
[138] Lai WH, Su YH, Teoh LG, Hon MH. Commercial and natural dyes as photosensitizers for a water-based dye-sensitized solar cell loaded with gold nanoparticles. J Photochem Photobiol A: Chem. 2008;195(2–3):307–13.
[139] Barazzouk S, Kamat PV, Hotchandani S. Photoinduced electron transfer between chlorophyll a and gold nanoparticles. J Phys Chem B. 2005;109(2):716–23.
[140] Calogero G, Di Marco G, Cazzanti S, Caramori S, Argazzi R, Di Carlo A, et al. Efficient dye-sensitized solar cells using red turnip and purple wild sicilian prickly pear fruits. Int J Mol Sci. 2010;11(1):254–67.
[141] Ghobashy MM, Mohamed TM. Radiation preparation of conducting nanocomposite membrane based on (copper/polyacrylic acid/poly vinyl alcohol) for rapid colorimetric sensor of mercury and silver ions. J Inorg Organomet Polym Mater. 2018;28(6):2297–305.
[142] Wang Y, Chen P, Liu M. Synthesis of well-defined copper nanocubes by a one-pot solution process. Nanotechnology. 2006;17(24):6000.
[143] Mirabi E, Akrami Abarghuie F, Arazi R. Integration of buildings with third-generation photovoltaic solar cells: a review. Clean Energy. 2021;5(3):505–26.
[144] Zhang Q, Jin L, Zhang Y, Zhang T, Li F, Xu L. *In situ* sulfidation of porous sponge-like $CuO/SiW_{11}Co$ into $Cu_2\ S/SiW_{11}Co$ as stabilized and efficient counter electrode for quantum dot-sensitized solar cells. Dalton Trans. 2021;50(13):4519–26.
[145] Malik MA, Malik SN, Alenad A. 11 Nanomaterials for solar energy. Sol Energy Convers Storage: Photochem Modes. 2015;10:219.
[146] Wang C-L. Development of earth-abundant materials and low-cost processes for solar cells. USA: The University of Texas at Austin; 2014.
[147] Zavaraki AJ, Liu Q, Ågren H. Solar cell sensitized with "green" InP-ZnS quantum dots: effect of ZnS shell deposition. Nano-Struct Nano-Objects. 2020;22:100461.
[148] Shabzendedar S, Modarresi-Alam AR, Noroozifar M, Mansouri-Torshizi H. Synthesis and characterization of poly (p-aminoazobenzene) nanosheet as a new derivative of polyaniline containing azo groups under green chemistry condition and its high efficiency in solar cell. Synth Met. 2019;255:116115.
[149] Xue Q, Xia R, Brabec CJ, Yip H-L. Recent advances in semi-transparent polymer and perovskite solar cells for power generating window applications. Energy Environ Sci. 2018;11(7):1688–709.
[150] Thakur VK, Ding G, Ma J, Lee PS, Lu X. Hybrid materials and polymer electrolytes for electrochromic device applications. Adv Mater. 2012;24(30):4071–96.
[151] Backler F, Wilson GJ, Wang F. Rational use of ligand to shift the UV-Vis spectrum of Ru-complex sensitiser dyes for DSSC applications. Radiat Phys Chem. 2019;161:66–71.
[152] Damrauer NH, Cerullo G, Yeh A, Boussie TR, Shank CV, McCusker JK. Femtosecond dynamics of excited-state evolution in $[Ru\ (bpy)_3]^{2+}$. Science. 1997;275(5296):54–7.
[153] Wallin S, Davidsson J, Modin J, Hammarström L. Femtosecond transient absorption anisotropy study on $[Ru\ (bpy)_3]^{2+}$ and $[Ru\ (bpy)(py)_4]^{2+}$. Ultrafast interligand randomization of the MLCT state. J Phys Chem A. 2005;109(21):4697–704.
[154] Li R. Coatings for metallic bipolar plates in high-temperature polymer electrolyte fuel cells. forschungszentrum Jülich GmbH. Zentralbibliothek; 2019.
[155] Chopra KL, Paulson PD, Dutta V. Thin-film solar cells: an overview. Progress in Photovoltaics: research and applications. 2004;12(2–3):69–92.
[156] Luo D, Nakata K, Fujishima A, Liu S. Photochemistry and photo-electrochemistry on synthetic semiconducting diamond. J Photochem Photobiol C: Photochem Rev. 2017;31:139–52.

[157] O'Regan B, Grätzel M. A low-cost, high-efficiency solar cell based on dye-sensitized colloidal TiO_2 films. Nature. 1991;353(6346):737–40.
[158] Lee MM, Teuscher J, Miyasaka T, Murakami TN, Snaith HJ. Efficient hybrid solar cells based on meso-superstructured organometal halide perovskites. Science. 2012;338(6107):643–7.
[159] Mann S, Harris I, Harris J. The development of urban renewable energy at the existential technology research center (ETRC) in Toronto, Canada. Renew Sustain Energy Rev. 2006;10(6):576–89.
[160] Collins J, Gourdin G, Qu D. Modern applications of green chemistry: renewable energy. Green chemistry. NY, United States: Elsevier; 2018. p. 771–860.
[161] Busi E, Maranghi S, Corsi L, Basosi R. Environmental sustainability evaluation of innovative self-cleaning textiles. J Clean Prod. 2016;133:439–50.
[162] Reichel A, Mortensen LF, Asquith M, Bogdanovic J, Union PO. Environmental impacts of production-consumption systems in Europe. Luxembourg: European Environment Agency; 2014.
[163] Capello C, Hellweg S, Badertscher B, Betschart H, Hungerbühler K. Environmental assessment of waste-solvent treatment options – part 1: the ecosolvent tool – environmental assessment of waste-solvent treatment options. J Ind Ecol. 2007;11:26–38.
[164] Štengl V, Bakardjieva S, Grygar TM, Bludská J, Kormunda M. TiO_2-graphene oxide nanocomposite as advanced photocatalytic materials. Chem Cent J. 2013;7(1):1–12.
[165] Stan MS, Badea MA, Pircalabioru GG, Chifiriuc MC, Diamandescu L, Dumitrescu I, et al. Designing cotton fibers impregnated with photocatalytic graphene oxide/Fe, N-doped TiO_2 particles as prospective industrial self-cleaning and biocompatible textiles. Mater Sci Eng C. 2019;94:318–32.
[166] Islas Garcia AB. Effective photocatalytic waste water treatment system using metal oxides semiconductors: a review. Finland: Centria University of Applied Sciences; 2021.
[167] Natarajan TS, Mozhiarasi V, Tayade RJ. Nitrogen doped titanium dioxide (N-TIO_2): synopsis of synthesis methodologies, doping mechanisms, property evaluation and visible light photocatalytic applications. Photochem. 2021;1(3):371–410.
[168] Gürses A, Açıkyıldız M, Güneş K, Gürses MS. Dyes and pigments: their structure and properties. Dyes and pigments. New York City, USA: Springer; 2016. p. 13–29.
[169] Troynikov O, Watson C, Jadhav A, Nawaz N, Kettlewell R. Towards sustainable and safe apparel cleaning methods: a review. J Environ Manag. 2016;182:252–64.